The influence of thermal evolution and the global carbon cycle on Earth's climate during the Archean Eon

Master Thesis

Author:
J. E. Prins

Supervisors:
Prof. dr. N. J. Mayne
Prof. dr. I. E. E. Kamp

University of Exeter

university of groningen

Abstract

Context: The atmospheric composition and temperature of the Archean eon are poorly constrained, since a lack of geophysical data makes it difficult to find sufficient proxies. The proxies we do have indicate that the climate was likely temperate for at least a part of the period even though the sun was only about 75% as luminous as it is now, and that life likely started during this eon. The long term geochemical carbon cycle, driven by the interior thermal evolution of the Earth, is a stabilising factor for the climate, and might have stabilised the Archean climate as well.
Aims: In this work, we investigate the influence of the thermal evolution and geochemical carbon cycle on the evolution of the climate during the Archean eon.
Methods: We use a long timescale 1D model that couples the thermal evolution and the carbon cycle to find values for the atmospheric CO_2 levels and heating through the surface due to cooling of the mantle. These values are then used as input for a 3D general circulation model that performs short timescale, detailed simulations to use as 'snapshot' images of three different moments in the Archean.
Results: We find that the heating through the surface due to mantle cooling is insignificant when compared to the solar irradiance at the surface. The CO_2 partial pressure decreases by a factor of four during the course of the Archean. This dampens the temperature increase caused by the increasing solar luminosity and prevents increased poleward heat transport
Conclusions: The geochemical carbon cycle was likely a stabilising factor in the Archean eon, keeping the temperatures low against the increasing solar luminosity. It therefore does not explain why the eon had temperate climates while the solar luminosity was lower than it is today. The resulting temperatures are low enough for the planet to be able to fall into a glaciation, which is consistent with the evidence that that happened a few times during the period.

Acknowledgements

Doing research and writing a thesis are not easy, I think I can safely say so now. Staring at minor code issues that halt your progress for two weeks, getting lost in a paper written by someone who seems to enjoy making their sentences as unreadable as possible, working all day only to produce three lines of text... As interesting as this project was, it was a frustrating job at times. Especially as someone whose passion lies in bringing science to specifically a non-scientific audience, it was quite a struggle sometimes to get to where I am now.

But I made it. And for that, I have quite a few people to thank. First and foremost, my supervisors Nathan and Inga, for guiding me through this process, being understanding when things weren't going to plan, and helping me find the excitement in the project at our weekly meetings. Nathan, thank you for letting me work with you in Exeter, your excitement made me feel very welcome, and your kindness made me feel safe. Inga, thank you for welcoming me back at Kapteyn, and for your always sharp feedback. To both of you, thank you for helping me do this interesting project.

I would like to thank Jake, for helping me understand and run even a small part of the huge model you use in Exeter, and for helping me with the many big and small questions I had along the way. Denis, thank you for answering my code-related questions, and for being a lovely office mate in my last few weeks abroad. I would also like to thank Mark, for letting me use his model for this project. I read his master's thesis when he was still working on that, and already found it very interesting back then. Working with the code myself now, felt like full-circle moment.

Doing this project abroad was one of the best decisions I've made so far. It's taught me a lot about myself, and has re-awakened my urge to travel. I felt welcomed by everyone in Exeter, in particular the amazing PhD and postdoc students of the astro group. The daily crosswords and weekly pub trips made me feel like a part of the group within a few weeks, and I've made some friends and memories I'll never forget.

Last but not least, I would like to thank my friends Eef and Ylse from home, for listening to my endless rave stories about my time in Exeter, and being there for me when I was homesick.

The past seven months have been an incredibly valuable experience, and as happy as I am that it's over now, I wouldn't have missed it for the world.

Contents

Chapter 1

Introduction

Over its lifetime, the Earth has in practice been many different planets: from a hellish world with magma oceans and frequent asteroid impacts in the very beginning (Goldblatt et al., 2010), to multiple periods of global glaciation (Kasting and Catling, 2003) and from an oxygen-poor world with only single cellular lifeforms around 3 billion years ago (Catling and Zahnle, 2020) to the oxygen rich world that saw an explosion in biodiversity and complex lifeforms around 500 million years ago (Zhuravlev and Riding, 2000). We have discovered all this by analysing, dating and comparing layers of rock on and below the surface, which show fingerprints of factors like the temperature, pressure and atmospheric composition at the time they were formed. These factors together make up the environment at that time, and layers of rock are therefore a useful way to get a glimpse into the environment billions of years ago.

One challenge with obtaining constraints on the Earth's climate history is that the geological record is not permanent. The layers of rock that are essential to this research are constantly being deformed, broken apart and destroyed through plate tectonics, the large-scale movement of continental and oceanic plates. Therefore, the further back in time we go, the sparser the information, and the harder it is to investigate the environment. However, there is another way to shed light on the Earth's deep past, namely through computational models. Using constraints gained from the geological record, computer models can help us understand how these environmental parameters work together, what kind of world they create and by what processes they are influenced. Bit by bit we're getting closer to understanding our home planet's past. Understanding this deep past of the Earth and its many environments helps us to not only understand the history of the planet itself, but through that also understand planet formation and earth-like exoplanets.

In this work, we will try to better understand one aspect of the early Earth's environment. We will look at the link between the long term geochemical carbon cycle and the climate during the Archean eon, a period starting 4.0 billion years ago and spanning about a third of the Earth's history. This carbon cycle, a process driven by the planet's interior evolution and plate tectonics, works as a thermostat for the climate on timescales of millions of years. We try to quantify its effect on the climate by combining a 1D model for the thermal evolution and carbon cycle with a more complex and short-timescale 3D General Circulation Model (GCM) of the atmosphere.

In section 1.1 we give a more detailed overview of the Archean eon and discuss some important open questions about the period. In section 1.2 we discuss the mechanisms of plate tectonics and mantle convection, and how they influence the climate through the carbon cycle. In section 1.3 we discuss meridional mass transport, which is an important factor in controlling the global climate. Section 1.4 is an overview of previous research that has been done into this topic and section 1.5 discusses the specific aims of this work and gives an overview of this thesis.

1.1 The Archean eon

The Archean eon is the period from 4.0 to 2.5 gigayears ago (Cohen et al., 2021). With the Earth being approximately 4.6 gigayears old, the era thus spans about a third of the planet's entire lifetime. The period is associated with the onset of primitive life, the onset of plate tectonics and the formation of the first continental crust. Its most distinguishing atmospheric characteristic is very low levels of oxygen, over a million times less than today (Catling and Zahnle, 2020).

The start of the Archean marked the end of the Hadean eon, an informal designation for the period directly after the formation of the Earth. The Hadean eon was characterised by a still solidifying crust, multiple periods of frequent asteroid impacts and the impact with another small planet that formed the Earth-Moon system (Goldblatt et al., 2010). Few to no rocks are found from this eon, as they have all been recycled by plate tectonics, so it is difficult to say more about the environment at that time.

Initially, the beginning of the Archean was defined as coinciding with the onset of life (Catling and Zahnle, 2020), but this might also have been shortly before or up to 500 million years after the start of the period (Knoll and Nowak, 2017). Due to this uncertainty in timing, the beginning was later defined to be the formation of the very first rocks and fixed at 4.0 gigayears ago, as the earliest well-preserved rocks date back to that time (Catling and Zahnle, 2020).

The ending of the Archean was set at the time of the Great Oxidation Event (GOE), when oxygen levels in the atmosphere rapidly rose. This event was initially dated to $\sim$2.5 Ga ago, but using newer proxies, that dating was later adjusted to after $\sim$2.4 gigayears ago. The ending of the Archean remained fixed at 2.5 Ga ago, and therefore the GOE now falls outside of the period (Catling and Zahnle, 2020). After the Archean ended, the Proterozoic eon begin, which is, with nearly 2 gigayears, the longest of the Earth's four eons, and is roughly bounded by the rise of atmospheric oxygen on one end, and the Cambrian explosion (541 million years ago) on the other (Maloof et al., 2010).

1.1.1 Open questions about the Archean

Even though the oldest rocks date back to the Archean, the geological record is sparse. It is therefore difficult to precisely characterise the environment and this has led to a few problems that have yet to be solved.

1.1.1.1 Faint Young Sun paradox and atmospheric composition

One of these problems is the Faint Young Sun (FYS) paradox. It has been shown that the Sun has increased in luminosity over its lifetime, and was therefore fainter in the past. At the beginning of the Archean, the Sun's luminosity was 74% of what it is today, and that increased to 82% of the current luminosity by the end of this period (Gough, 1981). With the atmospheric composition of present-day Earth, that would lead to a mean global surface temperature between 255 and 270K, below the freezing point of water (see Figure 1.1) and would therefore make the Earth fall into a full glaciation during the whole eon. However, there is strong evidence that there were in fact oceans of liquid water during at least parts of the Archean, which would suggest temperatures well above the freezing point of water. There is still debate about how warm it actually was, but the suggested mean temperatures range from a temperate 0-20°C to a hot 60°C, with a preference for the more temperate climate recently (Charnay et al., 2020).

At this point, the FYS paradox is no longer a paradox in the sense that there is a very simple and reasonable solution: planetary conditions were different. A different atmospheric composition with higher concentrations of greenhouse gases or a different planetary albedo due

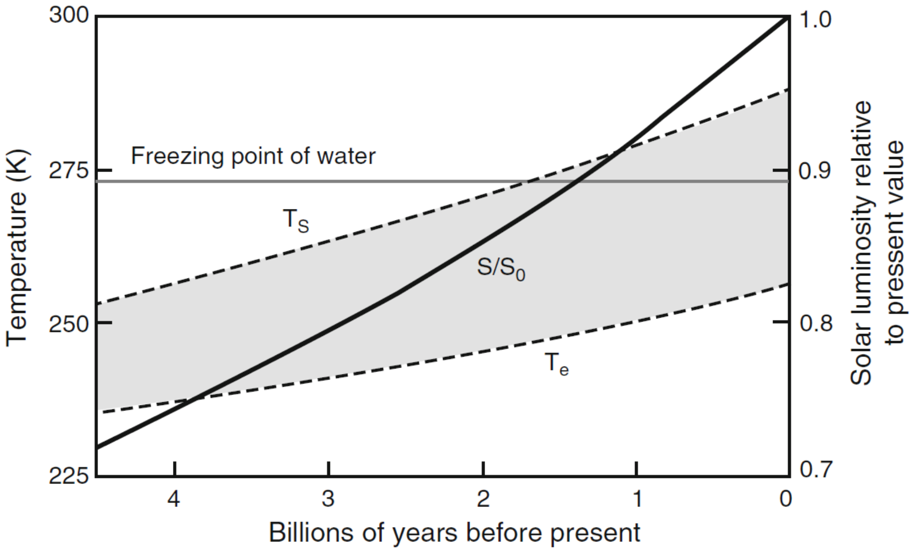

Figure 1.1: The Faint Young Sun paradox, taken from Güdel (2014), based on Kasting and Catling (2003). The solid black line shows the solar luminosity throughout the Earth's history, relative to today's value. The upper dashed line is the temperature assuming the atmosphere was the same as today. The lower dashed line is the temperature assuming no atmosphere. The solid grey line is the freezing point of water. It is clear from this figure that even with today's atmosphere, it would be too cold for liquid water to exist given the solar luminosity we had 4.0-2.5 billion years ago

to clouds and land distribution could easily solve the problem in theory. The range of possible greenhouse gas concentrations obtained from the available geological proxies are indeed in general higher than today's values, with for example CO_2 partial pressures between 3 and 750 mbar (Charnay et al., 2020) and CH_4 partial pressures between 0.01 and 10 mbar (Sauterey et al., 2020). The temperate climate needed to solve the paradox can be obtained with values that are within these constraints (Charnay et al., 2020), however the exact combination of factors that increased the global average temperature enough for liquid water to exist is still unknown. Therefore, though the problem is no longer a true paradox, it is not yet solved. Both geologists and climate scientists have been working on this for years, and a good overview of the current state of knowledge is given in Charnay et al. (2020)

1.1.1.2 Continents and plate tectonics

The Archean eon is generally regarded as the period in which plate tectonics started, although the exact timing is still unclear. As more evidence is gathered, this onset is shifted to earlier and earlier times and the current consensus over the past years has been that plate tectonics was in place by at least 3.2 gigayears ago (e.g. Mahapatro et al., 2012). However, recently studies have suggested that it might even have been in place around 4.0 gigayears ago (Windley et al., 2021). The onset of plate tectonics was most likely not an instantaneous event, but rather a slow transition that occurred regionally rather than everywhere at once (Sleep, 2007).

What the surface of the Earth looked like during that time is also still debated. There is evidence for the formation and break up of a few supercontinents, but those might also have been regular continents instead, or might not even have existed (e.g. de Kock et al., 2009; Nance et al., 2014; Bleeker, 2003; Piper, 2010). The total land fraction of the surface during that time might have been anything between 0% and 80% of what it is today (Krissansen-Totton et al., 2018).

Plate tectonics and the surface land fraction are important in this work, because they have a big influence on the climate, through the long term carbon cycle, which we will discuss in the next section.

1.2 The influence of plate tectonics and mantle convection on the climate

The processes of plate tectonics and mantle convection link the Earth's interior with the atmosphere through the long term geochemical carbon cycle. This section gives a brief overview of these processes and their influence on the climate. The information mostly follows Oosterloo (2020), unless otherwise specified.

1.2.1 The mechanics of plate tectonics and mantle convection

The outermost layer of the Earth, called the lithosphere, consists of multiple separate plates that slowly move with respect to one another. This process, which we call plate tectonics, causes continents to migrate across the surface of the Earth on long timescales, and is the reason why the distribution of land over the surface has been very different in the past.

The lithosphere consists of two separate layers, the crust and the upper layer of the mantle, that can be distinguished from one another by their chemical composition. The mantle is predominantly made up of iron and magnesium silicate minerals. The crust, on the other hand, consists of two types: continental crust composed mostly of granite and oceanic crust composed mostly of basalt (Earle, 2019). This distinction between continental and oceanic crust is vital in understanding the processes associated with plate tectonics. Continental crust is thick (~ 35 km) and buoyant, with an average density of about 2.7 g/cm^3 (Earle, 2019) and therefore very stable. It is on average 2 Gyr old, which makes it valuable for geological research (Cawood et al., 2013). Oceanic crust on the other hand is both thinner (~ 5 km) and denser ($\sim$3.0 g/cm^3) than continental crust (Earle, 2019), which makes it less stable. It is constantly being recycled, and is therefore seldom more than 200 million years old (Condie, 1997).

The formation and destruction of oceanic crust happens at mid-oceanic ridges and subduction zones respectively, and is illustrated in figure 1.2. At plate boundaries where oceanic and continental plates converge, called subduction zones, oceanic crust is subducted underneath the continental crust. The oceanic crust sinks, melts, and becomes part of the mantle. Far away from subduction zones, new oceanic crust is made at mid-oceanic ridges. Hot mantle rocks from the layer right beneath the lithosphere (the asthenosphere) are pushed upwards and melt due to the lower pressure, which allows them to become part of the lithosphere. They then move away from the mid-oceanic ridge, cool down and become denser.

This continuous movement of the oceanic crust away from mid-oceanic ridges and towards subduction zones is caused by convection in the asthenosphere. The asthenosphere is hotter than the lithosphere, with temperatures above 1500 K even in the upper layers. This high temperature allows the mantle to be deformed under sufficient stress and therefore act as a viscous fluid on timescales of millions of years, a phenomenon called solid-state creep. Heating from below, caused by cooling of the core, and cooling at the top create a temperature gradient within the mantle, which creates enough stress for the mantle to start convection, and this then acts as a conveyor belt for the tectonic plates on top.

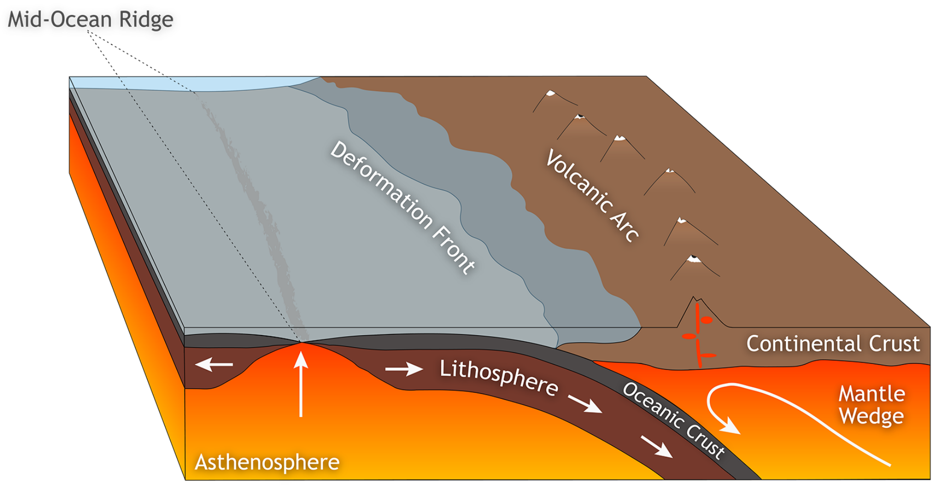

Figure 1.2: The life cycle of oceanic crust. Oceanic crust is formed at mid-oceanic ridges, where magma from the asthenosphere ascends to the surface and cools down. It is then slowly transported toward the ocean-continent plate boundary where it is subducted and recycled back into the mantle. Image credit: Roberto Molar Candanosa (`robertomolar.com/multimedia`).

1.2.2 The long term geochemical carbon cycle

Plate tectonics and mantle convection have an influence on the climate, because they are the main driving force behind the long term geochemical carbon cycle, also called the carbon-silicate cycle. This acts as a thermostat to the Earth over long timescales, as first suggested by Walker et al. (1981). The long term geochemcial carbon cycle is not to be confused with the short term biochemical carbon cycle that governs the distribution of carbon between the biosphere, hydrosphere, atmosphere and the Earth's surface (Kamiuto, 1994). Rather, the geochemical carbon cycle governs the distribution of carbon between the atmosphere, lithosphere and the Earth's interior and therefore dictates how much carbon is available for the biochemical carbon cycle.

In the geochemical carbon cycle, carbon is cycled between the atmosphere, land, ocean, seafloor and mantle, as can be seen in figure 1.3. CO_2 is taken out of the atmosphere by dissolution in rainwater. As this water reaches the surface, the CO_2 reacts with rocks in a process called silicate weathering (hence the name carbon-silicate cycle). Figure 1.3 shows this reaction for the silicate mineral wollastonite, but the reaction happens for other such minerals as well. This reaction becomes more efficient with increasing temperature, meaning that if the temperature increases, more CO_2 is taken out of the atmosphere.

CO_2 is a gas that is transparent to visible and ultraviolet radiation, while it absorbs infrared radiation. Solar radiation, being the strongest at visible wavelengths, is thus let through, whereas the thermal radiation from the Earth's surface is blocked by CO_2 in the atmosphere. CO_2 is therefore a greenhouse gas, meaning that a higher atmospheric CO_2 concentration causes higher temperatures. Thus, if increasing temperatures cause more CO_2 to be taken out of the atmosphere, this in turn decreases the temperature again, hence the thermostat-function of the carbon cycle.

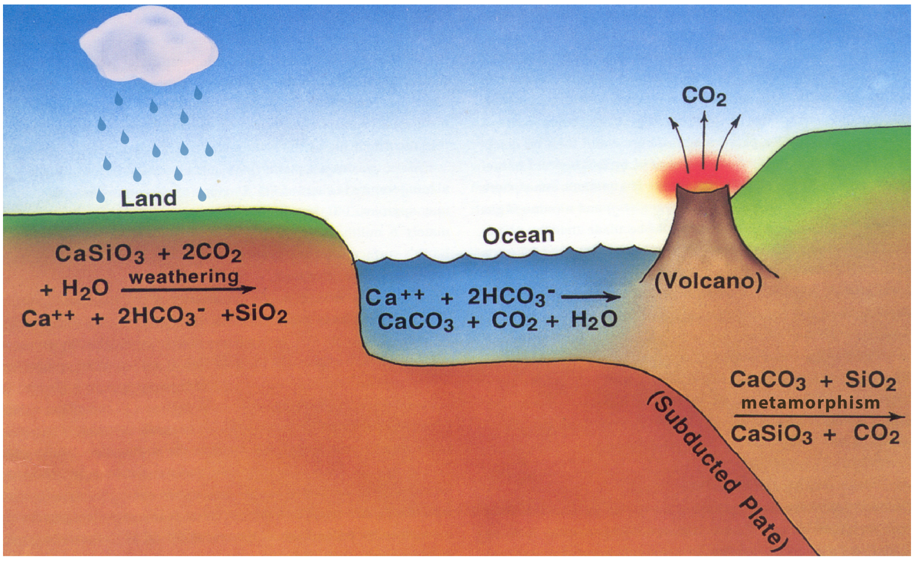

Figure 1.3: A schematic overview of the carbon-silicate cycle. CO_2 reaches the surface dissolved in rainwater. It reacts with silicate rocks, and the reaction products are transported to the ocean, where they react again to form carbonate and CO_2. Carbonate is stored on the oceanic crust and CO_2 reacts with the crust through seafloor weathering. Once it reaches a subduction zone, the carbonate undergoes metamorphism, releasing CO_2 again. This CO_2 is then either immediately outgassed from volcanoes, or subducted into the mantle to later be outgassed at mid-oceanic ridges. Image credit (modified): James F. Kasting (`personal.ems.psu.edu/~jfk4/PersonalPage/ResInt2.htm`), adapted from Kasting et al. (1993)

.

If the products of silicate weathering are then dissolved in river water, they are transported to the ocean, where they react to form carbonates and CO_2. The carbonates sink and are deposited on the seafloor to form sediments. Some of the CO_2 stays in the seawater, while the rest is taken up by the oceanic crust through a process called hydrothermal carbonisation, which acts as a form of seafloor weathering. This process is pH dependent (Krissansen-Totton and Catling, 2017), with lower pH leading to more effective weathering.

The carbon that is now stored in oceanic crust is transported to subduction zones through plate tectonics. Once the oceanic crust sinks under the continental crust, the increased pressure and temperature cause carbonate rocks to change through metamorphism, thereby releasing the carbon in the form of CO_2. This CO_2 is then either fully subducted and stored in the mantle, or immediately released back into the atmosphere through arc volcanism. Meanwhile, at mid-oceanic ridges, CO_2 that was stored in the mantle is released back into the ocean, while at the same time new weatherable rock is exposed.

The equilibrium of this cycle is dependent on factors like atmospheric temperature, ocean temperature and the speed with which oceanic plates move. In turn, it dictates the distribution of carbon over the atmosphere, lithosphere and the Earth's interior. Plate tectonics and the geochemical carbon cycle are thus inherently linked with the climate, and therefore with everything that happens above the surface of the Earth, including the development and evolution of life. Life, in turn, influences everything from atmospheric composition (e.g. Lyons et al., 2014) to plate tectonics and the building of mountain belts (Parnell and Brolly, 2021). Understanding the link between processes inside the Earth and processes on and above the surface is therefore crucial in understanding the history of both our own planet and others.

1.3 Meridional mass transport

Another important process controlling the overall climate is the heat transport due to general circulation in the atmosphere. On Earth, this circulation is driven by temperature gradients and the planet's rotation and is contained in three circulation cells per hemisphere, called Hadley cells, Ferrel cells and polar cells. Figure 1.4 shows a schematic overview of the present day Earth with these circulation cells.

On both sides of the equator, hot air near the surface becomes convectionally unstable and rises to the top of the troposphere, creating a low pressure zone near the equator. The risen air diverges poleward and this poleward movement causes the air to get closer to the rotational axis of the Earth. The resulting coriolis force then deflects the air eastward, creating jet streams. At latitudes of around 30° north and south, the eastward jets become so strong that the flow breaks down into eddies. This instability, combined with cooling due to radiation to space, causes the air to sink down toward the surface again and create a high pressure zone at these latitudes. The air then flows toward the low pressure zone near the equator and is deflected westward due to the coriolis force, creating the easterly (westward) trade winds. This closes the loop of the Hadley cell.

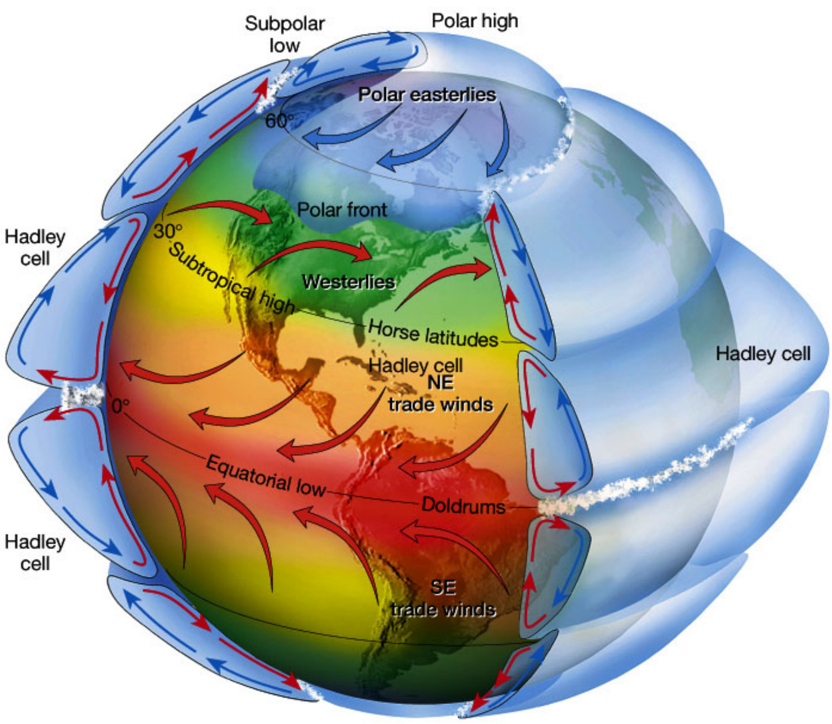

Figure 1.4: A schematic overview of the general circulation of present-day Earth, showing Hadley cells, Ferrel cells and polar cells as well as the corresponding high and low pressure zones. Image taken from Lutgens and Tarbuck (2001)

Something very similar happens near the poles, where warm air rises around latitudes of 60° north and south and flows toward the poles. Once cooled, it is dense enough to sink near the poles, and the resulting polar high pressure zone causes equatorward flow near the surface back to ∼60° latitudes, closing the loop of the polar cell. Again, because of the Coriolis force, this causes strong and consistent westward winds at these latitudes, and a strong eastward jet stream at the top of the troposphere and at higher latitudes.

In between these two cells is a region of baroclinic instability, where the strong eastward motion in the tropopause cannot be sustained, so the flow breaks down into large-scale eddies. There is no clear straightforward poleward flow of heat in these latitudes due to this instability, but the circular motions of the eddies do transport heat in the direction of the poles, and hence when averaged over longer periods of time, this latitudinal zone shows a circulation cell as well: the Ferrel cell. The Ferrel cell essentially functions as a gear that connects the Hadley and polar cells, to complete the general circulation in the atmosphere (Kushnir, 2000; Vallis, 2017).

This general circulation pattern is an important cause of heat transport from the equator to the poles. One way of visualising the circulation is using the meridional mass stream function, given by:

$$\Psi = -2\pi a \cos\phi \int_{surface}^{top\ of\ atmosph.} \overline{\rho v} \mathrm{d}z, \tag{1.1}$$

where a is the planet's radius, ϕ the latitude, ρ the air density, v the latitudinal velocity and z the vertical coordinate. The zonal average of ρv is taken, i.e. the average over longitudes. The absolute value of this stream function indicates how much mass is transported due to circulation, and the sign indicates the direction of transport.

1.4 Previous work on the carbon cycle and the Archean climate

Until the last few decades, research into the climate of the Archean Earth used to be restricted to the field of geology. Catling and Zahnle (2020) and Charnay et al. (2020) review our current understanding of this eon, giving an overview of what we know from the geological record. The atmospheric composition is still poorly constrained, with for example the partial CO_2 pressure (pCO_2) ranging from 3 to 750 mbar. Constraints on the temperature typically vary between 0°C and 20°C, though there is still debate about this. Some data even suggests temperatures as high as 60°C, but Charnay et al. (2020) argue that this is at odds with the evidence for partial and global glaciations (Wit and Furnes, 2016; Ojakangas and Hegde, 2014; Kasting and Howard, 2006). Even though these glaciation events might have been very short compared to the 1.5 billion years duration of the Archean, a transition from a warm 60°C climate to a complete snowball Earth would require major changes in the atmospheric composition caused by yet unknown mechanisms, and no evidence has been found for such mechanisms yet.

More recently, numerical simulations have started to play an important role in research surrounding the Archean climate. This started with Walker et al. (1981), who were the first to suggest that the geochemical carbon cycle involving temperature dependent silicate weathering might provide long term stabilisation of the Earth's climate. They made a model for the carbon cycle using simple parametrisations, and this model was later used and adapted multiple times to investigate the influence of this cycle on the early Earth's climate. One example of this is Tajika and Matsui (1992), who made a coupled thermal evolution and carbon cycle model to simulate the evolution of the Earth's atmosphere. They showed that the carbon cycle is indeed a stabilising factor and found Archean CO_2 levels that were 100-1000 higher than today's, resulting in the temperate climate needed to resolve the FYS paradox. Another example of early carbon cycle modelling is Sleep and Zahnle (2001), who used a long timescale carbon cycle model without coupled thermal evolution, and adapted that for the Archean. To simulate Archean circumstances, they assumed quicker plate tectonics, higher heat flows through the surface and more alkaline oceans. This last point is still strongly debated (e.g. Tajika and Matsui, 1992; Krissansen-Totton et al., 2018). The results of this model suggest that the Archean was cold unless there was another strong greenhouse gas, because the more vigorous plate tectonics and abundant weatherable impact ejecta from asteroid bombardments at the beginning of the Archean were an efficient CO_2 sink. However, it later turned out that in this model, the influence of seafloor weathering was likely overestimated because the authors fixed the pH to a value that is too alkaline, and they parametrised the seafloor weathering with a dependence on pCO_2, which in reality turned out to be weaker than previously thought. Instead, the temperature and pH dependence turned out to be the most important factors in determining the efficiency of seafloor weathering, as was found in another long term model of this kind, developed in Krissansen-Totton et al. (2018). The authors made a carbon cycle model for the early Earth including ocean chemistry using an empirically derived pH and temperature dependence of seafloor weathering from Krissansen-Totton and Catling (2017). They found that during the Archean, the ocean slowly became more alkaline (from a pH of $6.6^{+0.6}_{-0.4}$ to one of $7.0^{+0.7}_{-0.5}$). This turned out to be a result of the increasing solar luminosity, since that caused temperatures to rise, thus continental weathering to be more efficient and thus CO_2 levels to decrease, which then decreased the dissolution of atmospheric CO_2 into the ocean. However, the increased continental weathering did cause a larger influx of CO_2 into the ocean via rivers, which somewhat moderated the effect. They found average temperatures between 0 and 50°C and found that seafloor weathering was less dominant than assumed in Sleep and Zahnle (2001), which explains why the climate was a lot more temperate.

Even more recently, 3D General Circulation Models (GCMs) have been used to explore the Archean climate. These short timescale models calculate the circulation of matter in a planet's atmosphere on a 3D grid, and are often used for weather forecasting and climate research. Charnay et al. (2017) used such a model to simulate both the climate and the carbon cycle at 3.8 Ga ago, assuming an initial pCO_2 of 10-1000 mbar and then modelling the equilibrium temperatures. They also found that the carbon cycle keeps the climate temperate (8.5-30.5°C) without needing other greenhouse gases. Contrary to Krissansen-Totton et al. (2018), however, they did find that seafloor weathering was, at least initially, the dominant process and the climate was therefore insensitive to the land fraction. However, as more continental crust was formed and seafloor spreading slowed down, the continental weathering became more important.

All in all, both 1D and 3D models have been used to study the influence of the carbon cycle on the Archean climate. 1D models were often used to study the global long term evolution of the climate, whereas 3D simulations were used to study the climate in more detail, but only at specific moments during the eon.

1.5 Aim of this project

The aim of this project is to combine the two types of models: a long timescale box model for the thermal evolution and carbon cycle, comparable with those in Tajika and Matsui (1992), Sleep and Zahnle (2001) and Krissansen-Totton et al. (2018), and a short timescale 3D GCM in order to investigate in more detail how the Earth's interior has influenced the evolution of the climate throughout the Archean eon and what the consequences of this are for the big questions surrounding the early Earth. In combining these two models, we can study the evolution of the climate in more detail, rather than either studying the global, less detailed, evolution of the climate, or a detailed depiction of the climate at just one moment in time. Furthermore, this allows us to complement some simplifications that are made in the GCM, by allowing the atmospheric composition to change during the Archean and by implementing interior thermal evolution in our analysis.

As a long term model, we use the one developed in Oosterloo (2020), which couples the thermal evolution (through a parametrisation of mantle convection) to the geochemical carbon cycle to investigate the role of the planetary interior in the long term evolution of atmospheric CO_2 and habitability of exoplanets. This model was based on other models made for the Earth, and can hence easily be used for the Archean Earth.

The heat flux from the interior through the surface and the average CO_2 partial pressure obtained from this thermal evolution and carbon cycle model are then used as the input for a GCM. For that, we use the Unified Model (UM) developed by the MetOffice and adapted by the Exeter Exoplanet Theory Group (EETG) (`exoclimatology.com`) to work for various types of exoplanets, solar system planets and the early Earth. Because of its complexity, the UM can't run on long timescales and we therefore use it for short timescale, 'snapshot' simulations at various times during the Archean. This allows us to explore in more detail what the climate looked like at the time of those snapshots, rather than the global averages produced by just a box model.

In chapter 2, we discuss both models that are used more thoroughly and explain how we combine them to get our results. We then discuss these results in chapter 3, first for the thermal evolution model, then for the UM and finally in section 3.3 we summarise and discuss the interpretation of these results for the evolution of the climate. Lastly, chapter 4 is a discussion of the results in light of the broader context, previously done research and open questions, a discussion on the limitations of this project and an outlook on possible future work.

Chapter 2

Methodology

In this chapter, we discuss the two models that were used and how we used them. Section 2.1 gives an overview of the long timescale coupled thermal evolution and carbon cycle model, whereas section 2.2 gives an overview of the shorter timescale UM. Then finally, in section 2.3, we explain how both models were combined.

2.1 Long timescale thermal evolution and carbon cycle model

The long timescale model that combines the interior evolution of the Earth with the long term geochemical carbon cycle was developed by Oosterloo (2020), based on previous work by Schubert et al. (2001), Driscoll and Bercovici (2014), Höning et al. (2019) and Foley (2015). The model was created to investigate the role of plate tectonics in the long term evolution of carbon dioxide on earth-like exoplanets and Oosterloo (2020) used the model to assess how planetary mass, core size, radiogenic mantle heating, carbon abundance and land coverage influenced the geochemical carbon cycle and therefore the CO_2 pressure on these planets.

This section discusses the basic principles behind the model. A full mathematical derivation including the input parameters can be found in Oosterloo (2020) or the appendix of Oosterloo et al. (2021).

2.1.1 Thermal evolution

The first component of the model simulates the thermal evolution of the Earth's interior by solving the equations for temperature balance in the mantle. This model is based on those discussed in Schubert et al. (2001), Driscoll and Bercovici (2014) and Höning et al. (2019). The mantle is heated from below by cooling of the core through a lower thermal boundary layer, and from within by the decay of the radioactive isotopes ^{238}U, ^{235}U, ^{232}Th and ^{40}K. Furthermore, it is cooled by a heat flow to the surface through an upper thermal boundary layer.

The heating by radioactive isotopes is calculated by relating the modern-day heat flow of these isotopes to their half lives. The heat flows through the upper and lower thermal boundary layer can be related to the temperatures at the top and bottom of the mantle using the relation between the Nusselt and Rayleigh numbers, the Nu-Ra relation. The Nusselt number is given by:

$$Nu = \frac{\bar{q}}{q_c}, \tag{2.1}$$

and is the ratio of the total heat flow ($\bar{q}$) over the conductive heat flow (q_c), the latter of which can be written as:

$$q_c = \frac{k(T_l - T_u)}{D}, \tag{2.2}$$

with k the thermal conductivity, T_l the temperature at the lower boundary, T_u the temperature at the upper boundary and D the vertical thickness of the layer.

The Rayleigh number is given by:

$$Ra = \frac{g\alpha(T_l - T_u)D^3}{\kappa\nu}, \tag{2.3}$$

with g the gravitational constant, α the thermal expansivity, κ the thermal diffusivity of the material, ν the viscosity and the other variables the same as in equation 2.2. The Rayleigh number is a measure of the convective vigor of a fluid. It can be further written in terms of the mantle temperature by assuming a Newtonian rheology for the mantle, in which case the viscosity can be written as $\nu \propto \exp[1/T]$ following the Arrhenius law (Stevenson et al., 1983).

The Nusselt and Rayleigh numbers are related via the Nu-Ra relation, $Nu \propto Ra^{\beta}$ where β depends on the mantle geometry and rheology. In this work, we used $\beta = 1/3$ as that corresponds to the boundary layer model used in Oosterloo (2020).

If the Rayleigh number is above a certain threshold, called the critical Rayleigh number Ra_{cr}, then the fluid becomes unstable and convection occurs. By setting $Ra = Ra_{cr}$ in both the upper and lower boundary layer, one can relate the heat flow through these layers and the thickness of these layers to the temperature gradient and hence the temperature balance can be solved. For Earth's mantle, Ra_{cr} is thought to have values as low as 450 (Höning et al., 2019) or as high as 1100 (Schubert et al., 2001). Here, Ra_{cr} is set to 1100 to be consistent with Oosterloo (2020) and Schubert et al. (2001).

2.1.2 Carbon cycle model

The second component, a carbon cycle model, is based on the model by Foley (2015), which in turn is based on the one from Sleep and Zahnle (2001). It solves a set of mass conservation equations for the various carbon reservoirs R_o (ocean), R_a (atmosphere), R_k (oceanic crust) and R_m (mantle).

Because the timescale to reach an equilibrium between the ocean and atmosphere reservoirs is much smaller than the timescale on which the other reservoirs reach an equilibrium ($\sim 10^3$ yr versus $\sim 10^6 - 10^9$ yr) (Sleep and Zahnle, 2001), these two reservoirs are treated as one in solving the mass balance. Then after each timestep, the steady-state values of the ocean and atmosphere reservoirs are calculated. It is assumed that the CO_2 in the ocean and atmosphere behaves as an ideal gas, in which case the atmospheric CO_2 partial pressure is directly dependent on the ocean reservoir via Henry's law (Foley, 2015). Furthermore, by simply using the ideal gas law, one can relate the CO_2 partial pressure to the atmospheric reservoir as well, therefore obtaining a relation between the ocean and atmospheric reservoirs.

The various relevant fluxes are the subduction flux of oceanic crust at subduction zones (F_{sub}, the outgassing flux caused by arc volcanism (F_{arc}), the outgassing flux at mid-oceanic ridges (F_{ridge}), the seafloor weathering flux (F_{sfw}) and the continental weathering flux ($F_{weather}$). F_{sub} and F_{arc} can be related because F_{arc} is a fraction of F_{sub}. This fraction is poorly constrained, and is therefore set at 0.5 for the model in Oosterloo (2020) and hence also for the model we used here. Furthermore, half of $F_{weather}$, which in principle takes carbon out of the atmosphere/ocean reservoir, is put back into that reservoir because with the formation of carbonate, half of the carbon is released back in the form of CO_2. Therefore for every two moles of CO_2 taken out of the atmosphere by continental weathering, only one mole is actually taken out of the atmosphere/ocean reservoir.

One important factor in the parametrisation of the fluxes is the dependence of $F_{weather}$ on the surface temperature, the one feature of the thermal evolution and carbon cycle that makes it such an effective thermostat. For this, the temperature is needed, which is calculated by linking the surface temperature to the CO_2 partial pressure, the planetary albedo and the solar luminosity via a simple parametrisation derived by Walker et al. (1981), which assumes CO_2 is the only relevant greenhouse gas.

Furthermore, just like the heating by radioactive isotopes, the parametrisations of F_{sfw} and $F_{weather}$ are scaling laws which scale the fluxes to present-day Earth fluxes.

2.1.3 Coupling of the thermal evolution to the carbon cycle

The coupling of the thermal evolution model to the carbon cycle model is done in two ways. First of all, in the carbon cycle model, F_{sub}, F_{ridge} and F_{sfw} all depend on the plate speed, the speed with which oceanic crust moves. This plate speed is coupled to the Rayleigh number by relating it to the horizontal flow speed of the upper thermal boundary layer, i.e. the upper part of the mantle, which is directly dependent on the Rayleigh number.

Furthermore, another link between the two models is made because the heat flow through the upper thermal boundary layer is dependent on the surface temperature, and hence on the CO_2 pressure. Therefore, not only does the interior thermal evolution influence the carbon cycle, but the carbon cycle in turn also influences the interior thermal evolution.

2.1.4 Using the model for the Archean eon

Since the coupled thermal evolution and carbon cycle model was calibrated to present-day Earth values and since it was primarily made to investigate the influence of factors like planetary mass, core size and radioactive isotope abundance, there are some caveats to using it for the early Earth.

First and foremost, it is still unsure when and how plate tectonics started, see for a more detailed discussion section 1.1.1.2. Recent studies have suggested that plate tectonics as we know it might have been around by the beginning of the Archean (Windley et al., 2021), but it could just as well be that the processes worked differently or were in place only in certain regions (Sleep, 2007; Windley et al., 2021). The model we use assumes that plate tectonics was already in place from the start, and that it has always worked in the same way.

Secondly, Oosterloo (2020) has shown that the land fraction has a big influence in the coupling of the thermal evolution and the carbon cycle, with a land fraction of zero completely decoupling the two systems. As discussed in section 1.1.1.2, the land fraction in the Archean was likely lower than it is now, but the exact value is not known. In the thermal evolution and carbon cycle model that we used, we assumed a constant land fraction that is the same as today's. Furthermore, the planetary albedo was likely different during the Archean than it is now, since that is dependent on the land fraction. Again, we assumed an albedo that is constant and the same as today's.

2.2 Short timescale climate model (Unified Model)

The more complex, short timescale model we used is the Unified Model (UM), a general circulation model (GCM) developed by the UK MetOffice for both weather and climate applications. Since 2014, it has been adapted to work for a range of different types of exoplanets, most notably hot Jupiters (e.g. Mayne et al., 2017), mini-Neptunes/Super Earths (e.g Mayne et al., 2019) and terrestrial planets (e.g. Eager et al., 2020). More recently, the model has been adapted for Martian (McCulloch et al., 2021) and early Earth applications, the latter of which we have used for this work.

The UM consists of various components working together. The most important of these are the dynamical core, the radiative transfer scheme and the interaction between the surface and the atmosphere. This section gives a brief overview of these components.

2.2.1 Dynamical core

The basis of any GCM is a dynamical core that models the circulation of mass in the atmosphere of a planet. It does this by integrating a set of differential equations that describe the motion of a fluid over time. This set of equations typically includes one equation for mass conservation, a set of equations for momentum balance (the Navier Stokes equations) and one equation for energy balance.

The dynamical core of the UM is called ENDGame (Even Newer Dynamics for General atmospheric modelling of the environment). ENDGame is based on the non-hydrostatic, deep-atmosphere, fully compressible equations, that is, equations which describe an atmosphere that is not in hydrostatic equilibrium, that can have a depth comparable to the planetary radius and where fluid parcels can change in density (Staniforth and Wood, 2003, 2008). The core solves these equations on a latitude-longitude grid using a semi-implicit scheme, in which the solution for each timestep is a weighted average of the solutions obtained by the explicit and implicit mehtods. The implicit method is in this case based on the Crank-Nicolson scheme (Crank and Nicolson, 1947), which is a form of a trapezoidal method of integration.

Furthermore, the integration scheme is semi-Lagrangian. Lagrangian integration traces the trajectories of individual fluid parcels, whereas Eulerian integration traces the properties of a fluid as it flows through a fixed grid. The problem with Lagrangian integration is that parcels can start to cluster together, leaving large regions of space empty. To prevent this, a semi-Lagrangian integration defines fluid particles according to an Eulerian grid, performs the integration over one timestep, interpolates the properties of the fluid on the Eulerian grid and then redefines the fluid particles according to that same fixed grid. This can potentially violate the mass conservation, but ENDGame uses a scheme (developed in Wood et al., 2014) that is inherently mass conserving (Mayne et al., 2014).

2.2.2 Radiative tranfer

The other crucial aspect of any GCM is the radiative transfer scheme, which calculates how radiation of different wavelengths is reflected, absorbed, transmitted and emitted by the atmosphere. This radiative transfer scheme distinguishes between so-called shortwave and longwave radiation, where the former is the stellar radiation, i.e. the radiation that is either directly originating from the Sun or reflected by the atmosphere, and the latter is so-called planetary radiation, that has been emitted by the Earth's surface or atmosphere. There is in reality some overlap in wavelength between the two types of radiation, but in general stellar radiation has shorter wavelengths (peak around 0.5 μm) than the planetary radiation (peak around 10 μm), hence the names shortwave and longwave radiation.

The UM uses a radiative transfer scheme called Suite Of Community RAdiative Transfer codes based on Edwards and Slingo (SOCRATES) (Edwards and Slingo, 1996; Manners et al., 2015). It uses the correlated-k method as discussed in Lacis and Oinas (1991), where wavelength intervals with similar spectral properties are grouped and treated as one to decrease computational cost. We used the configuration from Walters et al. (2019), where the longwave radiation is treated via 12 bands between 3.3 μm and 10 mm and shortwave radiation is treated via 29 bands between 0.2 and 10 μm.

2.2.3 Surface

In the UM simulations we performed, the Earth was assumed to be a fully ocean-covered planet. The surface was therefore considered to be a an ocean with a single 2.4 m thick mixed layer, based on Frierson et al. (2007), which interacts with the atmosphere by reflecting, absorbing and emitting radiation, but has no exchange of matter with the atmosphere. It was assumed that there is no horizontal heat transport within the ocean. Furthermore, in this treatment ice formation in the ocean when temperatures fall below the freezing point, so there is no ice albedo feedback.

2.3 Combined carbon cycle and climate modelling

We combined the two different models by using the interior heat flux and CO_2 partial pressures obtained from the thermal evolution and carbon cycle model as input for the UM. We ran the thermal evolution and carbon cycle model using the parameters in table 2.1. Note that in this table, three different initial mantle temperatures are given. We ran the model for each mantle temperature separately, to explore a range of values. Furthermore, we ran the model with present-day Earth land fraction and albedo and assumed that all carbon is in the atmosphere/ocean reservoir initially, since pCO_2 values were likely high on the early Earth (Payne et al., 2020). We used the Nu-Ra relation exponent mentioned in section 2.1. We ran the model for two different solar luminosity scenarios: one where it was kept constant at the value it had at the beginning of the Archean (74% of its modern day value), and one where it was allowed to change according to the parametrisation given in Gough (1981).

Parameter	Description	Value(s)	Unit
$T_m(0)$	Initial mantle temperature	1600, 1800, 2000	K
$R_s(0)/R_{tot}(0)$	Initial fraction of carbon in ocean/atmosphere	1	-
a	Albedo	0.31	-
f_{land}	Land fraction	0.3	-
β	Nu-Ra relation exponent	1/3	-
Ra_{cr}	Critical Rayleigh number	1100	-
f	Subduction zone CO_2 degassing fraction	0.5	-

Table 2.1: Relevant parameters for the thermal evolution and carbon cycle model. All other input parameters can be found in Oosterloo (2020).

The two results from the thermal evolution and carbon cycle model that are relevant for this research are the atmospheric CO_2 levels and the interior heating through the surface caused by mantle cooling. These values were taken at the beginning (4.0 Ga ago), middle (3.25 Ga ago) and end (2.5 Ga ago) of the Archean and then used as input for the UM, by treating the interior heating as a heat flux from below and adding the CO_2 partial pressure to the initial atmospheric composition. This way we created detailed ‘snapshot’ images of those three moments. As mentioned in section 2.2, the Earth was treated as an ocean planet in the UM, and therefore, contrary to what we do in the thermal evolution and carbon cycle model, the land fraction was set to 0 for the UM. Other relevant input parameters for the UM are given in Table 2.2. We deliberately kept methane levels on the low side compared to constrains mentioned in Catling and Zahnle (2020), in order to more easily isolate the impacts of the CO_2 concentration on the climate. The day length was kept at 24 hours even though it was likely shorter in the past, and the eccentricity of the Earth’s orbit and axial tilt were both put to 0 for simplicity.

Parameter	**Name**	**Value(s)**	**Unit**
pCH_4	Methane partial pressure	0.1	mbar
d	Day length	24	h
e	Eccentricity of Earth’s orbit	0	-
θ	Axial tilt of Earth	0	°

Table 2.2: Relevant parameters for the UM runs.

To properly disentangle the influence of increasing solar luminosity on the climate from the influence of the thermal evolution and carbon cycle, we ran the UM for three scenarios. In the first scenario, the solar luminosity increased according to Gough (1981), but there was no evolution in the heating from the interior or in the CO_2 levels, we call this scenario LumChange. In the second scenario, the solar luminosity again increased, but now the interior heating and CO_2 levels were also allowed to change, we call this BothChange. In the third scenario, which we call CO2Change, the solar luminosity was kept constant, but the interior heating and CO_2 levels were allowed to change, in this case taking the output from the carbon cycle model run with constant solar luminosity. Table 2.3 gives an overview of the three scenarios

Scenario	**Solar luminosity**	**Interior heating and CO_2 levels**
LumChange	Changes	Stay constant
BothChange	Changes	Change
CO2Change	Stays Constant	Change

Table 2.3: An overview of the three scenarios for which the UM will be run.

All in all, we performed nine simulations with the UM, for three scenarios at three times during the Archean, using output parameters from the thermal evolution and carbon cycle model as input.

Chapter 3

Results

In this chapter, we discuss the results from both models that were used. First, in section 3.1, we discuss the heat flow through the surface and the evolution of atmospheric CO_2 levels, both results from the thermal evolution and carbon cycle model. In section 3.2, we discuss the result from the UM for the temperature and heat transport in the three scenarios discussed in section 2.3. Then finally, in section 3.3 we analyse and interpret the results to synthesise a complete picture of how the increasing solar luminosity and the presence of a carbon cycle influenced the evolution of the Archean climate.

3.1 Interior heating and CO_2 levels from the carbon cycle model

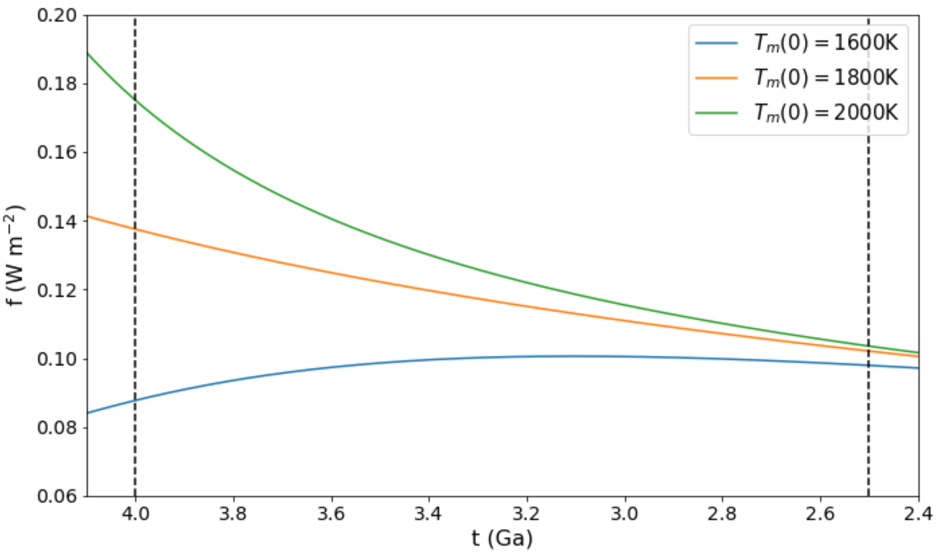

Figure 3.1: Surface heating from the interior caused by mantle cooling. The heat flux is shown for initial mantle temperatures of 1600K, 1800K and 2000K in blue, orange and green respectively. The vertical black dashed lines indicate the beginning and end of the Archean.

First of all, the thermal evolution and carbon cycle model was run for the three different initial mantle temperatures discussed in section 2.3. The other relevant input parameters can be found in Table 2.1.

The CO_2 partial pressure and the heat flux to the surface caused by cooling of the mantle can have a relevant influence on the clime. The former influences the radiative properties of the atmosphere and therefore the heat distribution, whereas the latter functions as a heat source from below.

Figure 3.1 shows the heat flux from the interior through the surface for the three different mantle temperatures. This flux could be regarded as a source of heat from below in the UM, rather than the solar heat which comes from above. However, Figure 3.1 shows that the heating to the surface was between 0.08 and 0.19 Wm^{-2} during the Archean. Considering that the current solar irradiance that reaches the surface of the Earth is typically between 60 and 300 Wm^{-2}, and was only 18-26% lower during the Archean (Gough, 1981), it is clear that the interior is an insignificant source of heat, and it will therefore be neglected from here on.

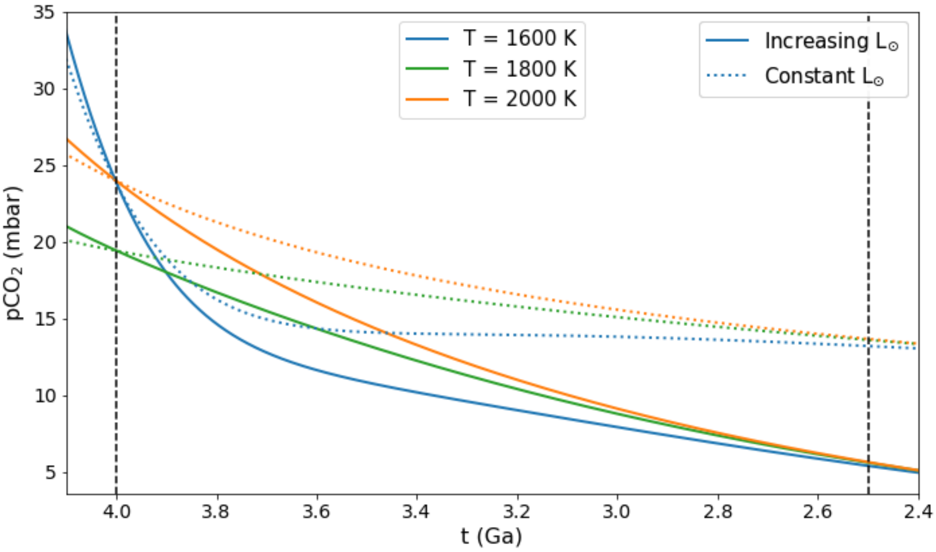

Figure 3.2: CO_2 partial pressure during the Archean. As in figure 3.1, initial mantle temperatures of 1600K, 1800K and 2000K are used, in blue, orange and green respectively. The solid lines show pCO_2 for an increasing solar luminosity according to Gough (1981), and the dotted lines show pCO_2 for a constant solar luminosity of 74% of its present-day value. The vertical black dashed lines show the beginning and end of the Archean.

The CO_2 partial pressure throughout the Archean is shown in Figure 3.2, again for three different initial mantle temperatures. In this figure, the CO_2 partial pressure is shown for two different scenarios as well. In one scenario, we allow the solar constant to increase according to Gough (1981), while in the other, we keep the solar constant at 74% of its current value, that is, the value it had at the beginning of the Archean according to Gough (1981).

Figure 3.2 shows a couple of things. First of all, in the scenario where the solar luminosity increases, the CO_2 partial pressure decreases by a factor of around 4 during the course of the Archean, from 22 mbar at 4.0 Ga ago to 5.6 mbar at 2.5 Ga ago when averaged over the initial mantle temperatures. This is a significant decrease, and it is therefore interesting to investigate its influence on the climate. If the solar luminosity remains constant however, the partial pressure also decreases, but less so, from 22 mbar at 4.0 Ga ago to 14 mbar at 2.5 Ga ago. This is an interesting test case to disentangle the effects of the solar luminosity and changing CO_2 levels. In both cases, the initial mantle temperature is most relevant in the first half of the period, and becomes less important later on, as the partial pressure converges toward the end of the period.

For the UM input, we used the average pCO_2 over the three initial mantle temperatures at the three moments in the Archean. In general, we see the values for pCO_2 vary between 5.6 mbar and 22 mbar during the Archean eon. This is within the geological constraints mentioned in the reviews by Charnay et al. (2020) and Catling and Zahnle (2020) (3-750 mbar), although they are on the lower end of that range.

Table 3.1 shows the pCO_2 input values for the various runs of the UM, for the three scenarios discussed in section 2.3. The pCO_2 level is an input parameter that is the same throughout the whole atmosphere. Further key input parameters for the UM are given in table 2.2,

Time	**LumChange**	**BothChange**	**CO2Change**
4.0 Ga ago	22 mbar	22 mbar	22 mbar
3.25 Ga ago	22 mbar	11 mbar	16 mbar
2.5 Ga ago	22 mbar	5.6 mbar	14 mbar

Table 3.1: pCO_2 values for the various UM runs, taken from Figure 3.2 and for the three scenarios discussed in section 2.3. The second column shows pCO_2 values for an increasing solar luminosity, without thermal evolution and carbon cycle (LumChange), the third column shows values for increasing solar luminosity, but with thermal evolution and carbon cycle (BothChange), and the fourth column shows values for a constant solar luminosity, with thermal evolution and carbon cycle (CO2Change).

3.2 Climate evolution from the Unified Model

3.2.1 Temperature and climate regime

Figure 3.3 shows the global average temperatures for the three moments in the Archean and for the three scenarios. Temperature maps can be found in appendix A. Figure 3.3 shows that in both scenarios with increasing solar luminosity (LumChange and BothChange, resp. blue and orange in the figure), the average temperature increases, though it increases more rapidly in the LumChange scenario (from 2°C to 10°C) than in the BothChange scenario (from 2°C to 4.5°C). In the CO2Change scenario (green) with a constant solar luminosity, the overall temperature decreases slightly, because the atmospheric CO_2 levels decrease while everything else is kept constant. We can conclude that the increasing solar luminosity has the largest effect on the global average temperature. After all, the overall temperature increases even if we allow the CO_2 levels to decrease. However, the decreasing CO_2 levels do have a dampening effect on this temperature rise.

Figure 3.4 shows the equator-to-pole temperature difference and the pole and equator temperatures separately, again for the three moments in the Archean and for the three different scenarios. In the scenario without thermal evolution and carbon cycle but with increasing solar luminosity (LumChange), the temperature at the poles increases with 27K, while the temperature at the equator increases with only 10K. The equator-to-pole temperature difference therefore decreases with 17K. On the other hand, in the scenario with a carbon cycle (BothChange), the temperatures at the equator and pole change with 3K and 5K respectively, resulting in a decrease in equator-to-pole temperature difference of only 2K. This shows that in the LumChange scenario, heat transport from the equator to the poles is significantly more efficient than in the BothChange scenario. The increasing solar luminosity makes the heat transport from equator to poles more efficient, and decreasing CO_2 levels cancel that effect out to a large extent. In the next section, we try to figure out why that happens, which processes are involved in the heat

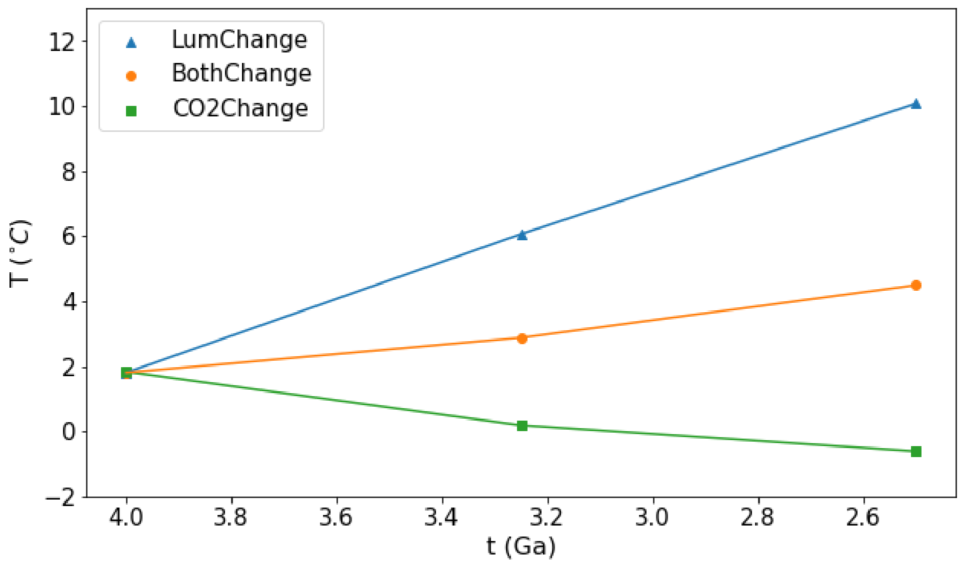

Figure 3.3: The global average temperature over the course of the Archean in the various scenarios. The blue triangles show the scenario with increasing solar luminosity and without thermal evolution and carbon cycle (LumChange), the orange circles show the scenario with increasing solar luminosity and a thermal evolution and carbon cycle (BothChange), and the green squares show the scenario with constant solar luminosity but with thermal evolution and carbon cycle (CO2Change). Lines between the datapoints are based on interpolation.

transport and whether it is purely a result of overall increasing temperatures or if the CO_2 levels also play a role.

3.2.2 Heat transport from equator to poles

3.2.2.1 Meridional mass transport

As discussed in section 1.3, the heat transport due to general circulation in the atmosphere is an important process controlling the overall climate. Figure 3.5 shows the meridional mass stream function for both scenarios where the solar luminosity increases (LumChange and BothChange). Blue means that the circulation is counterclockwise, whereas red means that the circulation is clockwise. From this point onward, we no longer consider the scenario with constant solar luminosity (CO2Change), since we are primarily interested in the influence of the thermal evolution and carbon cycle on the background of the increasing solar luminosity. Figure 3.5 shows that without a carbon cycle (3.5a), the Hadley and Ferrel cells become higher, wider and stronger over time, with the Hadley cells growing from approximately 15 km to approximately 18 km altitude and from spanning approximately 25° to spanning approximately 30° on either side of the equator. This suggests more displacement of mass from the equator to the poles, and therefore more efficient heat transport. In the case with a carbon cycle (3.5b), the cells grow a bit as well, but a lot less.

Although the meridional heat transport is an important part of the climate, other heating processes such as shortwave and longwave radiation also play a role. To get a full picture of the entire system, we need to look at all of the heating processes.

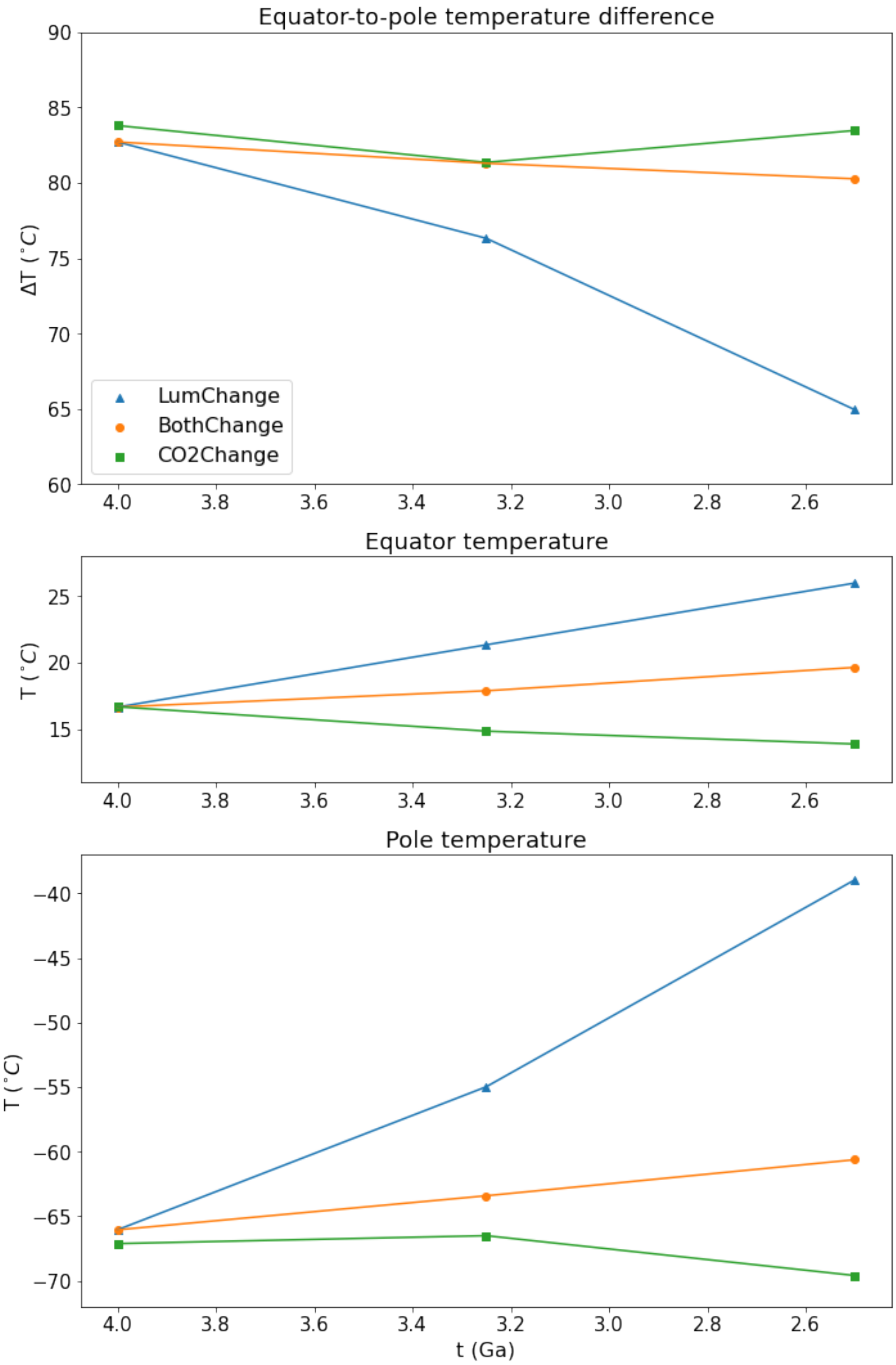

Figure 3.4: The equator-to-pole temperature difference and equator and pole temperatures over the course of the Archean in the various scenarios. The blue triangles show the scenario with increasing solar luminosity and without thermal evolution and carbon cycle (LumChange), the orange circles show the scenario with increasing solar luminosity and a thermal evolution and carbon cycle (BothChange), and the green squares show the scenario with constant solar luminosity but with thermal evolution and carbon cycle (CO2Change). Lines between the datapoints are based on interpolation.

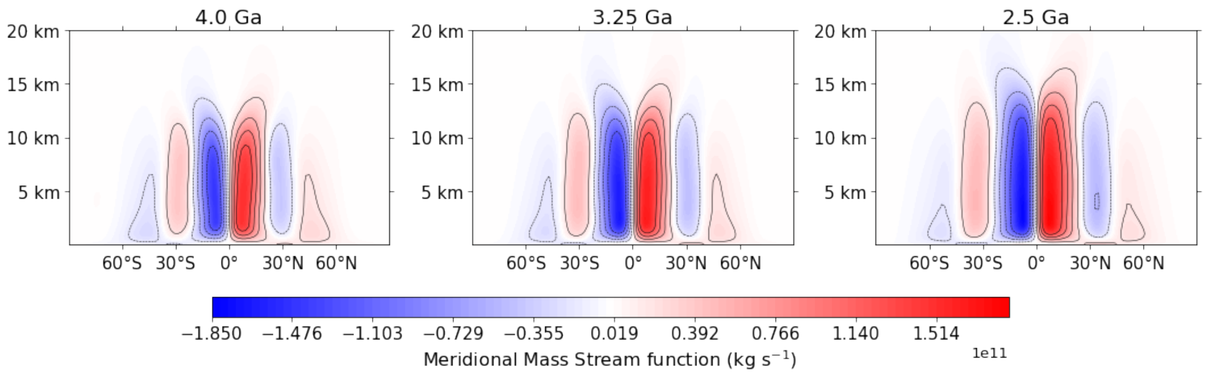

(a) Without thermal evolution and carbon cycle

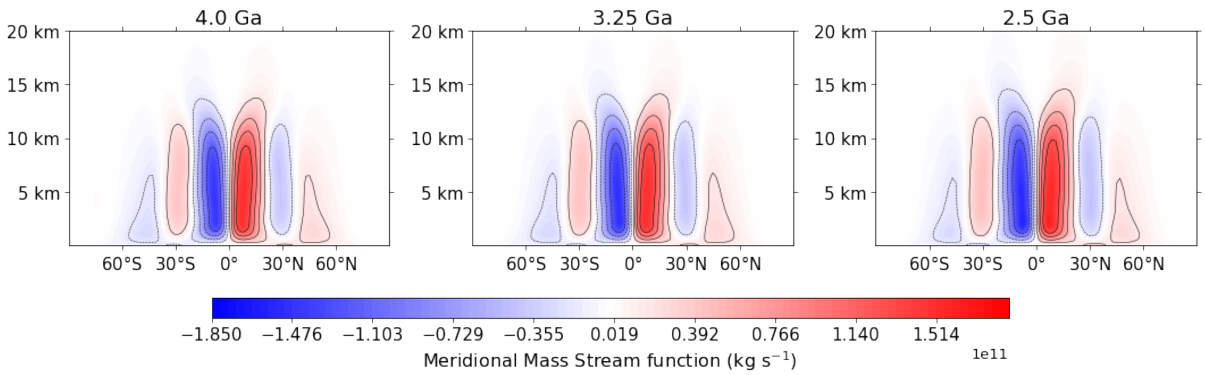

(b) With thermal evolution and carbon cycle

Figure 3.5: Meridional mass stream functions for the two scenarios with increasing solar luminosity, LumChange and BothChange.

3.2.2.2 Other heating processes

To assess the relative importance of various heating processes, the daily change in temperature due to specific processes is plotted. Figure 3.6 shows the various heating processes as a function of altitude in one of our simulations, as an example. It shows the average change in temperature per day, but the sum of all of the processes at any altitude is always zero. This is the case for three reasons: because the data is only considered after the system has reached an equilibrium, because the data is averaged over longitude (taking out the day/night effect) and because there is no seasonality, nor any other external factors that change the temperature from day to day. Therefore, rather than showing how much these processes actually change the temperature, these plots show how much different processes contribute to keeping the temperature stable, and therefore how important different processes are at certain latitudes and altitudes.

Not all of these processes are relevant for the heat transport from the equator to the poles. Figures 3.8 and 3.7 show a selection of processes, for the equator and poles respectively. In this case, the equator spans from 10°S to 10°N and the poles span from 75° to 90° on both hemispheres. For the poles, the relevant processes are longwave radiation and advection, whereas for the equator, the relevant processes are longwave radiation, advection, shortwave radiation and convection. These processes were selected because they are the ones with a significant effect on the temperature in the troposphere, see appendix B for the data on all processes. Furthermore, these figures show the three moments we have simulated during the Archean simultaneously.

The difference between convection and advection means different things in different contexts.

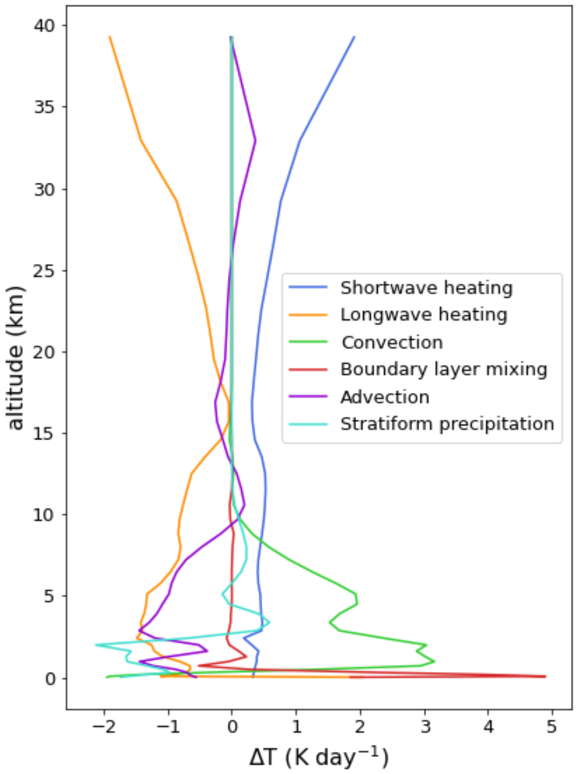

Figure 3.6: The change in temperature per day as function of altitude at the equator (between 10°S and 10°N) 4.0 Ga ago. Each solid line shows the temperature change due to one heating or cooling process. The sum over all processes at any altitude is always zero, since the climate is stable and the temperature changes are zonally averaged.

In this case, the difference is due to the resolution of the model we used. The flow of matter that is calculated as a result of pressure gradients in each timestep is classed as advection. However, some flows will work on scales smaller than the used grid, or on timescales shorter than the used timestep, and will thus not be picked up by the model. These flows, classed as convection, are treated by a parametrisation after the advection step, and will thus show up differently in the figures.

Figure 3.7 shows the two processes at the poles. The main source of heating in the troposphere is advection, i.e. bulk displacement of mass, which is balanced by cooling due to longwave radiation, so the heat is transported to the poles by mass displacement, and is then radiated away. Without thermal evolution and a carbon cycle (3.7a), i.e. with a constant level of CO_2, both of these processes increase in strength over the Archean. Furthermore, the processes increase in reach, that is, the effects stretch to higher altitudes. With a carbon cycle, however, the strength of these two processes seems to stay almost exactly the same. Therefore we conclude that at the poles, the heating due to mass displacement increases with increasing solar luminosity, but this effect is cancelled when CO_2 levels decrease due to the carbon cycle.

It is also interesting to look at what happens near the equator, the place where the heat originates. Figure 3.8 shows that tropospheric heating is mainly caused by convection, i.e. warm air rising from the surface upwards, and a little bit by stellar (shortwave) radiation. This is balanced by cooling due to advection and longwave radiation. We also see that the convection, advection and longwave radiation strongly increase in strength and height over the Archean when

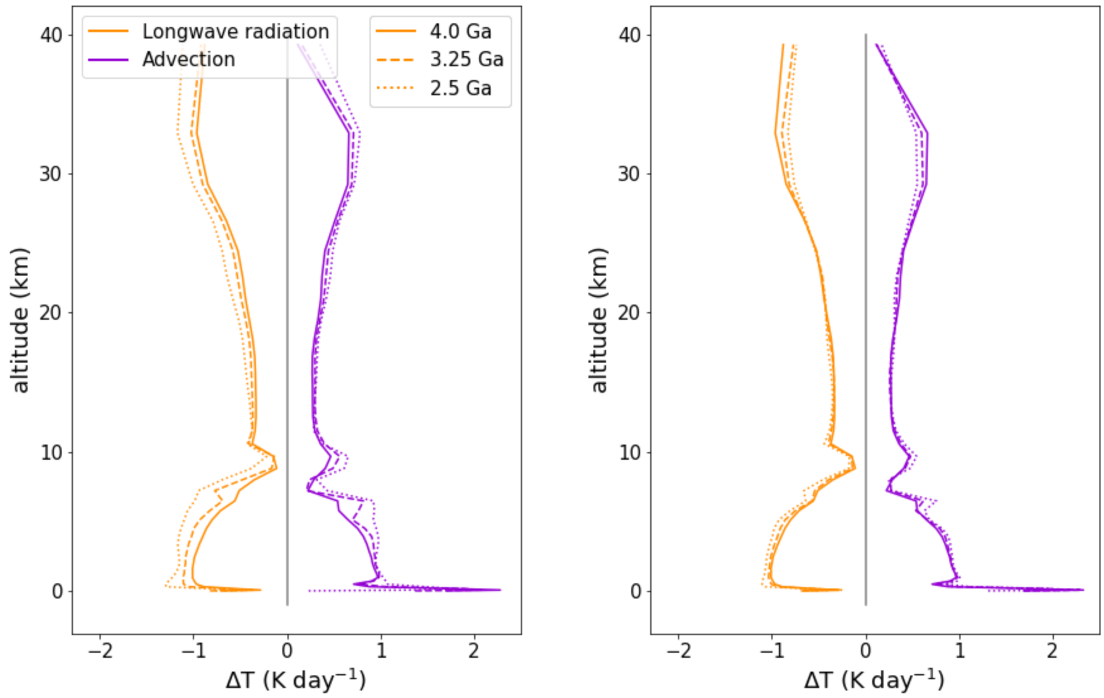

(a) Increasing solar luminosity, without thermal evolution and carbon cycle (LumChange)

(b) Increasing solar luminosity, with thermal evolution and carbon cycle (BothChange)

Figure 3.7: The daily change in temperature as function of altitude due to longwave radiation and advection at the poles

there is no carbon cycle, which happens less so in the case with a carbon cycle. This is consistent with what we found in section 3.2.2.1, because Figure 3.5 also showed that the Hadley and Ferrel cells become larger and stronger in time without a carbon cycle, while staying roughly constant with a carbon cycle. This meridional mass transport shows up as convection and advection in Figure 3.8.

The temperature change due to shortwave radiation high up in the atmosphere stays constant without a carbon cycle, while it decreases with a carbon cycle. This heating is almost entirely balanced by the cooling due to longwave radiation. On the other hand, the temperature change due to shortwave radiation below a latitude of 20 km increases slightly without a carbon cycle, while it stays more or less constant with a carbon cycle.

3.3 Summary and interpretation of results

Let us summarise and interpret what we have found in the previous sections. We have combined two models to quantify the influence of the thermal evolution and carbon cycle on the Archean climate.

Surface heating due to cooling of the mantle is insignificant when compared to the solar irradiance at the surface, even with the lower solar luminosity we had in the Archean. It is therefore not a relevant factor to consider for the Archean climate. The atmospheric CO_2 levels we found are consistent with geological constraints mentioned in Charnay et al. (2020) and Catling and Zahnle (2020), and they change significantly over the course of the eon due to the

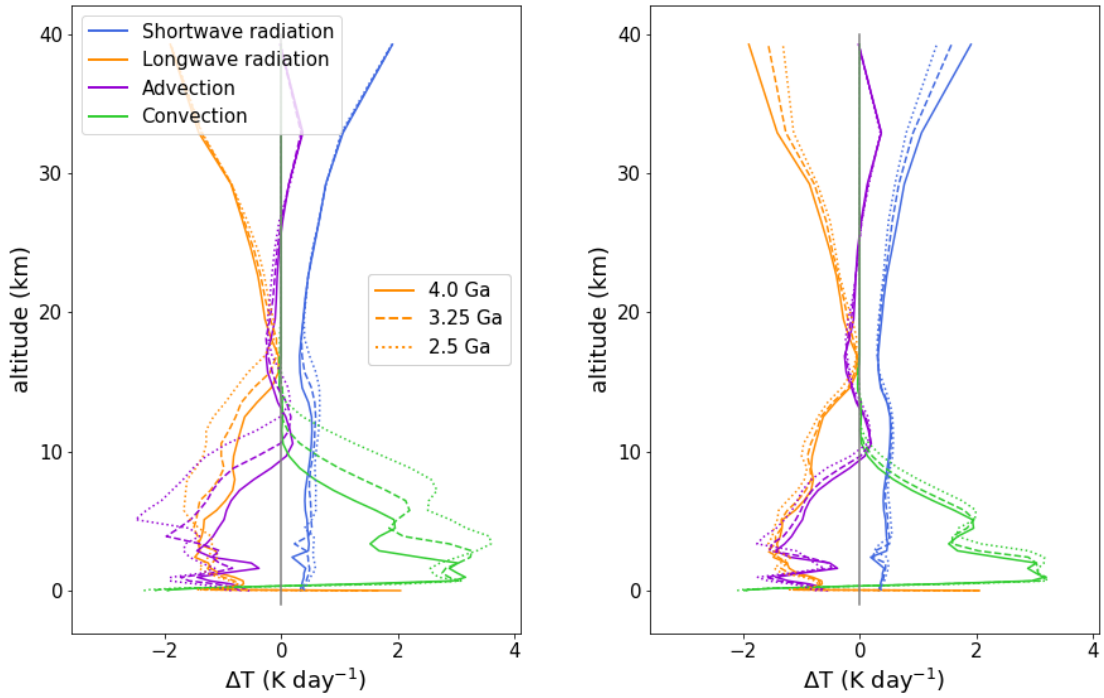

(a) Increasing solar luminosity, without thermal evolution and carbon cycle (LumChange)

(b) Increasing solar luminosity, with thermal evolution and carbon cycle (BothChange)

Figure 3.8: The daily change in temperature as function of altitude due to longwave radiation, shortwave radiation, convection and advection at the poles

Earth's thermal evolution and carbon cycle. If we let the solar luminosity increase, the CO_2 partial pressure decreases by a factor of 4 over 1.5 billion years, whereas it decreases by a factor of 1.6 if we assume a constant solar luminosity.

Next, we used the UM to determine the effect of this CO_2 decrease over the course of the Archean. It turned out that the thermal evolution and carbon cycle dampen the average temperature increase caused by the strengthening Sun, but not enough to keep the temperature completely stable or even cause cooling. It does, however, almost completely cancel the heat transport from the equator to the pole.

This increase in heat transport to the poles when CO_2 levels remain constant primarily happens in the form of mass transport. The convective cells, explained in section 1.3, strengthen due to the increased surface temperatures at the equator, and hence bring more warm air poleward. If the thermal evolution and carbon cycle are turned on and CO_2 levels are allowed to decrease, the temperature at the equator is largely stabilised and there is thus less heat transport through mass displacement, so the temperature difference between the equator and poles remains larger.

All in all, we can say that over the course of the 1.5 billion years of the Archean eon, the thermal evolution and carbon cycle are an effective way of keeping the climate stable against the backdrop of an increasing solar luminosity, since they cause the atmospheric CO_2 levels to decrease.

Chapter 4

Discussion and conclusion

4.1 Implications of results

We have found that the carbon cycle is a stabilising factor in the climate of the Archean eon, which mitigates most of the heating caused by the increasing solar luminosity from the beginning to the end of the Archean, as found in previous research as well (e.g. Sleep and Zahnle, 2001; Tajika and Matsui, 1992; Krissansen-Totton et al., 2018). It keeps temperatures, especially at the poles, relatively stable when compared to the scenario without a carbon cycle. Since it prevents temperatures from rising, it is not a factor that would solve the FYS paradox, but rather one that makes solving the problem more challenging.

We saw that the global average temperature had values between 2°C and 4.5°C for the scenario with increasing solar luminosity and changing atmospheric CO_2 levels. This is consistent with most of the geological constraints. Evidence for oceans of liquid water suggest temperatures above 0°C. Though some oxygen isotope ratios even suggest hot oceans of 50°C to 85°C (Knauth, 2005), others suggest temperatures below 40°C (Hren et al., 2009; Blake et al., 2010). Furthermore, there are alternative interpretations to the data presented in Knauth (2005) as well (Catling and Zahnle, 2020). Temperature limits on the formation of certain minerals suggests temperatures of $<$18°C (Hardie, 1967; Buick and Dunlop, 1990), constraining the temperature even further to lower values. Methane levels were deliberately kept low as explained in section 2.3, so an increase with a factor of ten might increase the temperature by another few degrees, while still remaining within the geological constraints (J. K. Eager, personal correspondence, November 29, 2021).

The average polar temperatures that we found were well below the freezing point (between -66°C and -38°C), meaning that the ocean in those regions would be covered in ice. This is consistent with glacial rocks that have been found from various moments in the Archean (Wit and Furnes, 2016; Nhleko, 2003; Ojakangas and Hegde, 2014), which serve as evidence for the existence of extended ice sheets. At the poles in particular, the difference between the scenarios with and without a carbon cycle at the end of the Archean were big, around 25°C. Heat transport from the equator to the poles becomes significantly more efficient with a higher solar luminosity, but that effect is mitigated if the CO_2 levels decrease. Therefore, at the end of the Archean, ice sheets would extend to much lower latitudes in the presence of a carbon cycle than in the scenario without. Important to note here is that glaciation of the polar regions would increase the planet's albedo and hence decrease the temperature even further, but ice albedo feedback was beyond the scope of this research. Therefore the effect of introducing a CO_2 cycle would in reality be even bigger.

The temperate climate that we found means that any life living at or near the surface of the planet should be mesophilic, i.e. preferring temperatures between 0°C and 40°C. Reconstructions based on phylogenetic data of the earliest biological samples indicate that this is reasonable (Boussau et al., 2008; Cantine and Fournier, 2018). However similar research suggests life started in hot environments instead (Gaucher et al., 2008; Garcia et al., 2017). This could be explained by the relatively common theory that life started in local hot environments like hydrothermal vents or the impact craters of large asteroids (Boussau et al., 2008; Abramov and Mojzsis, 2009).

4.2 Limitations of the approach and future work

In this section we will discuss the most important of limitations of our approach, and their expected impact on the results.

First, there still exist large uncertainties around plate tectonics and the emergence of land at the beginning of the Archean, as was also discussed in section 1.1.1.2. This would influence the results of the thermal evolution and carbon cycle model. It might be that plate tectonics had not yet started at the beginning of the eon, or that it was only functioning regionally. Since plate tectonics is one of the crucial driving factors of the carbon cycle, this would of course influence the results. Less effective plate tectonics in the beginning of the Archean would mean both less subduction of carbonates into the mantle and less weatherable new ocean crust, hence a less efficient carbon cycle and higher atmospheric CO_2 values. On the other hand, if plate tectonics was more rigorous in the Archean, as suggested by Sleep and Zahnle (2001), the carbon cycle might be more efficient, causing CO_2 values to be lower instead and therefore temperatures higher. The unknown, changing and likely lower land fraction plays into this as well. Less land means less CO_2 uptake through continental silicate weathering (Oosterloo, 2020), and therefore higher atmospheric CO_2 levels and higher temperatures. Furthermore, our treatment of land in the thermal evolution and carbon cycle model was inconsistent with that in the UM, since we treated the Earth as an ocean planet in the latter. Land in the UM would likely mainly increase the planetary albedo (thereby decreasing the temperature) and influence the atmospheric circulation.

One important feedback that was not considered in the thermal evolution and carbon cycle model is the temperature and pH dependence of seafloor weathering. We treated the seafloor weathering flux with a power law pCO_2 dependence, but that dependence is weak, and the seafloor weathering rate is more strongly dependent on ocean temperature and pH, as discussed in Krissansen-Totton and Catling (2017). Krissansen-Totton et al. (2018) argue that including ocean chemistry, therefore letting the seafloor weathering rate depend on temperature and pH, would increase global temperatures and stabilise the climate even further against increasing solar luminosity.

A factor that could have influenced the efficiency of silicate weathering but was not considered in this work, is the abundant impact ejecta caused by the late heavy bombardment. Asteroid impacts expose new weatherable rocks and Sleep and Zahnle (2001) have shown that this further decreases temperatures. Furthermore, different types of continental and oceanic crust material also influence the weathering rates, as discussed in e.g. Fabre et al. (2011).

In the thermal evolution and carbon cycle model, the only factor that directly influenced the surface temperature is the CO_2 partial pressure. However, in reality there are of course many other factors that influence the temperature, like other greenhouse gases, changing albedo and atmospheric circulation. Because none of these other factors are considered in the thermal evolution and carbon cycle model, but some of them are in the UM, this yields different surface temperatures for one model when compared to the other. To be more specific, surface temperatures from the UM are higher than those from the thermal evolution and carbon cycle model.

This means that the thermal evolution and carbon cycle model likely underestimates the surface temperature, and therefore overestimates the CO_2 levels, which in turn causes an overestimation of surface temperatures in the UM.

One crucial factor that was not considered in the UM, already mentioned in the previous section, is ice albedo feedback. Sea ice strongly increases a planet's albedo, and since our results show a temperate to cold climate with sub-zero temperatures at the poles, that coud have significantly altered our results, decreasing the temperature even more as also discussed in Kienert et al. (2012). This is consistent with the previously discussed evidence of multiple periods of partial or complete glaciation (e.g. Wit and Furnes, 2016; Nhleko, 2003; Ojakangas and Hegde, 2014).

Finally, some factors concerning the Earth's movement in its orbit around the Sun have not been considered. First and foremost, the Earth's rotational period was likely shorter in the past. We know that the Moon has been slowly drifting away from the Earth, so to preserve angular momentum in the system, the Earth's rotation must have slowed down and days were therefore shorter in the past. Estimations based on sedimentary cyclic rhythmites (Williams, 2000) and orbit modelling (Bartlett and Stevenson, 2016) indicate day lengths between 10 and 20 hours. This faster rotation would increase the coriolis force, causing poleward flow to break down into eddies sooner and hence reducing the efficiency of heat transport from the equator to the poles. This would further reduce the temperature at the poles in all of our scenarios. Furthermore, we assumed the Earth's orbit was circular and that there was no obliquity in the Earth's rotational axis, therefore ignoring any seasonal effects.

One factor that was also not considered in this work is the influence of life on the carbon cycle. Research (e.g. Lovelock and Margulis, 1974; Nicholson et al., 2018) suggests that life can play a crucial factor for stabilising the climate in such a way that it stays habitable. For example, organisms like CH_4 producing methanogens could keep global temperatures higher than they otherwise would be (Lenton, 1998). On the other hand, Lenton et al. (2012) and Feulner et al. (2015) discuss the possibility of metabolic evolution destabilising the carbon cycle and therefore throwing the whole planet into a glaciation during the Neoproterozoic and Paleozoic eras, causing mass extinctions. This line of research was well beyond the scope of this work, but is definitely interesting to furter look into, especially if we extend it to other planets and the search for extraterrestrial life.

4.3 Conclusion

In this work, we have combined two different types of climate models that work on different timescales to investigate the influence of the geochemical carbon cycle on the evolution of the Archean climate. We found that the main consequence of the carbon cycle is stabilisation of the climate against temperature increase due to an increasing solar luminosity. This stabilisation is realised because the carbon cycle takes CO_2 out of the atmosphere, a process that becomes more efficient at higher temperatures. Global average temperatures are between 2°C and 10°C, which indicates that any surface-dwelling organisms must be mesophilic. Furthermore, the carbon cycle prevents significant heating of the polar regions by preventing an increase in bulk mass displacement from the equator to the poles. This keeps the equator to pole temperature difference higher, since the poles are colder and that in turn makes glaciations more likely.

Bibliography

O. Abramov and S. J. Mojzsis. Microbial habitability of the hadean earth during the late heavy bombardment. *Nature*, 459:419–422, 5 2009. ISSN 00280836. doi: 10.1038/nature08015.

B. C. Bartlett and D. J. Stevenson. Analysis of a precambrian resonance-stabilized day length. *Geophysical Research Letters*, 43:5716–5724, 6 2016. ISSN 19448007. doi: 10.1002/2016GL068912.

R. E. Blake, S. J. Chang, and A. Lepland. Phosphate oxygen isotopic evidence for a temperate and biologically active archaean ocean. *Nature*, 464:1029–1032, 4 2010. ISSN 00280836. doi: 10.1038/nature08952.

W. Bleeker. The late archean record: A puzzle in ca. 35 pieces. *Lithos*, 71:99–134, 2003. ISSN 00244937. doi: 10.1016/j.lithos.2003.07.003.

B. Boussau, S. Blanquart, A. Necsulea, N. Lartillot, and M. Gouy. Parallel adaptations to high temperatures in the archaean eon. *Nature*, 456:942–945, 12 2008. ISSN 00280836. doi: 10.1038/nature07393.

R. Buick and J. Dunlop. Evaporitic sediments of early archaean age from the warrawoona group, north pole, western australia. *Sedimentology*, 37:241–277, 1990.

M. D. Cantine and G. P. Fournier. Environmental adaptation from the origin of life to the last universal common ancestor. *Origins of Life and Evolution of Biospheres*, 48:35–54, 3 2018. ISSN 15730875. doi: 10.1007/s11084-017-9542-5.

D. C. Catling and K. J. Zahnle. The archean atmosphere. *Science Advances*, 6, 2020. URL `http://advances.sciencemag.org/`.

P. A. Cawood, C. J. Hawkesworth, and B. Dhuime. The continental record and the generation of continental crust. *Bulletin of the Geological Society of America*, 125:14–32, 1 2013. ISSN 00167606. doi: 10.1130/B30722.1.

B. Charnay, G. L. Hir, F. Fluteau, F. Forget, and D. C. Catling. A warm or a cold early earth? new insights from a 3-d climate-carbon model. *Earth and Planetary Science Letters*, 474: 97–109, 9 2017. ISSN 0012821X. doi: 10.1016/j.epsl.2017.06.029.

B. Charnay, E. T. Wolf, B. Marty, and F. Forget. Is the faint young sun problem for earth solved? *Space Science Reviews*, 216, 8 2020. ISSN 15729672. doi: 10.1007/s11214-020-00711-9.

K. Cohen, D. Harper, and P. Gibbard. Ics international chronostratigraphic chart 2021/10, 2021. URL `https://stratigraphy.org/`.

K. C. Condie. *Plate Tectonics and Crustal Evolution*. Elsevier, 4 edition, 1997. ISBN 9780750633864. doi: 10.1016/B978-0-7506-3386-4.X5000-9.

J. Crank and P. Nicolson. A practical method for numerical evaluation of solutions of partial differential equations of the heat-conduction type. *Mathematical Proceedings of the Cambridge Philosophical Society*, 43:50–67, 1947. ISSN 14698064. doi: 10.1017/S0305004100023197.

M. O. de Kock, D. A. Evans, and N. J. Beukes. Validating the existence of vaalbara in the neoarchean. *Precambrian Research*, 174:145–154, 10 2009. ISSN 03019268. doi: 10.1016/j.precamres.2009.07.002.

P. Driscoll and D. Bercovici. On the thermal and magnetic histories of earth and venus: Influences of melting, radioactivity, and conductivity. *Physics of the Earth and Planetary Interiors*, 236: 36–51, 11 2014. ISSN 00319201. doi: 10.1016/j.pepi.2014.08.004.

J. K. Eager, D. J. Reichelt, N. J. Mayne, F. H. Lambert, D. E. Sergeev, R. J. Ridgway, J. Manners, I. A. Boutle, T. M. Lenton, and K. Kohary. Implications of different stellar spectra for the climate of tidally locked earth-like exoplanets. *Astronomy and Astrophysics*, 639, 7 2020. ISSN 14320746. doi: 10.1051/0004-6361/202038089.

S. Earle. *Physical Geology - 2nd Edition*. BCcampus, Sep 2019. ISBN 978-1-77420-028-5. URL `https://opentextbc.ca/physicalgeology2ed`.

J. M. Edwards and A. Slingo. Studies with a flexible new radiation code. i: Choosing a configuration for a large-scale model. *Quarterly Journal of the Royal Meteorological Society*, 122: 689–719, 4 1996. ISSN 00359009. doi: 10.1002/qj.49712253107.

S. Fabre, G. Berger, and A. Nédélec. Modeling of continental weathering under high-co2 atmospheres during precambrian times. *Geochemistry, Geophysics, Geosystems*, 12, 10 2011. ISSN 15252027. doi: 10.1029/2010GC003444.

G. Feulner, C. Hallmann, and H. Kienert. Snowball cooling after algal rise. *Nature Geoscience*, 8:659–662, 10 2015. ISSN 17520908. doi: 10.1038/ngeo2523.

B. J. Foley. The role of plate tectonic-climate coupling and exposed land area in the development of habitable climates on rocky planets. *Astrophysical Journal*, 812, 10 2015. ISSN 15384357. doi: 10.1088/0004-637X/812/1/36.

D. M. Frierson, J. Lu, and G. Chen. Width of the hadley cell in simple and comprehensive general circulation models. *Geophysical Research Letters*, 34, 9 2007. ISSN 00948276. doi: 10.1029/2007GL031115.

A. K. Garcia, J. W. Schopf, S. I. Yokobori, S. Akanuma, and A. Yamagishi. Reconstructed ancestral enzymes suggest long-term cooling of earth's photic zone since the archean. *Proceedings of the National Academy of Sciences of the United States of America*, 114:4619–4624, 5 2017. ISSN 10916490. doi: 10.1073/pnas.1702729114.

E. A. Gaucher, S. Govindarajan, and O. K. Ganesh. Palaeotemperature trend for precambrian life inferred from resurrected proteins. *Nature*, 451:704–707, 2 2008. ISSN 14764687. doi: 10.1038/nature06510.

C. Goldblatt, K. J. Zahnle, N. H. Sleep, and E. G. Nisbet. The eons of chaos and hades. *Solid Earth*, 1:1–3, 2010. doi: 10.1146/annurev.astro.41.082201. URL `www.solid-earth.net/1/1/2010/`.

D. O. Gough. Solar interior structure and luminosity variations. *Sol. Phys.*, 74(1):21–34, Nov 1981. ISSN 1573-093X. doi: 10.1007/BF00151270.

M. Güdel. *Faint Young Sun Paradox*, pages 1–7. Springer Berlin Heidelberg, 2014. doi: 10.1007/978-3-642-27833-4_1700-5.

L. A. Hardie. The gypsum—anhydrite equilibrium at one atmosphere pressure1. *American Mineralogist*, 52:171–200, 2 1967. ISSN 0003-004X.

M. T. Hren, M. M. Tice, and C. P. Chamberlain. Oxygen and hydrogen isotope evidence for a temperate climate 3.42 billion years ago. *Nature*, 462:205–208, 11 2009. ISSN 00280836. doi: 10.1038/nature08518.

D. Höning, N. Tosi, and T. Spohn. Carbon cycling and interior evolution of water-covered plate tectonics and stagnant-lid planets. *Astronomy and Astrophysics*, 627, 7 2019. ISSN 14320746. doi: 10.1051/0004-6361/201935091.

K. Kamiuto. A simple global carbon-cycle model, Aug 1994. ISSN 0360-5442.

J. F. Kasting and D. Catling. Evolution of a habitable planet. *Annual Review of Astronomy and Astrophysics*, 41:429–463, 2003. ISSN 00664146. doi: 10.1146/annurev.astro.41.071601.170049.

J. F. Kasting and M. T. Howard. Atmospheric composition and climate on the early earth. *Philosophical Transactions of the Royal Society B: Biological Sciences*, 361:1733–1741, 10 2006. ISSN 09628436. doi: 10.1098/rstb.2006.1902.

J. F. Kasting, D. P. Whitmire, and R. T. Reynolds. Habitable zones around main sequence stars. *Icarus*, 101:108–128, 1 1993. ISSN 00191035. doi: 10.1006/icar.1993.1010.

H. Kienert, G. Feulner, and V. Petoukhov. Faint young sun problem more severe due to ice-albedo feedback and higher rotation rate of the early earth. *Geophysical Research Letters*, 39, 12 2012. ISSN 19448007. doi: 10.1029/2012GL054381.

L. P. Knauth. Temperature and salinity history of the precambrian ocean: Implications for the course of microbial evolution. *Palaeogeography, Palaeoclimatology, Palaeoecology*, 219:53–69, 4 2005. ISSN 00310182. doi: 10.1016/j.palaeo.2004.10.014.

A. H. Knoll and M. A. Nowak. The timetable of evolution. *Evolutionary Biology*, 3, 5 2017. doi: 10.1126/sciadv.1603076. URL `https://www.science.org/doi/10.1126/sciadv.1603076`.

J. Krissansen-Totton and D. C. Catling. Constraining climate sensitivity and continental versus seafloor weathering using an inverse geological carbon cycle model. *Nature Communications*, 8, 5 2017. ISSN 20411723. doi: 10.1038/ncomms15423.

J. Krissansen-Totton, G. N. Arney, and D. C. Catling. Constraining the climate and ocean ph of the early earth with a geological carbon cycle model. *Proceedings of the National Academy of Sciences of the United States of America*, 115:4105–4110, 4 2018. ISSN 10916490. doi: 10.1073/pnas.1721296115.

Y. Kushnir. The climate system: General circulation and climate zones, 2000. URL `https://web.archive.org/web/20040822022845/http://eesc.columbia.edu/courses/ees/climate/lectures/gen_circ/index.html`.

A. A. Lacis and V. Oinas. A description of the correlated-k distribution method for modelling nongray gaseous absorption, thermal emission, and multiple scattering in vertically inhomogeneous atmospheres. *Journal of Geophysical Research, vol. 96, p. 9027-9064 (1991)*, 96:9027, May 1991. ISSN 0148-0227. doi: 10.1029/90JD01945.

T. M. Lenton. Gaia and natural selection. *Nature*, 394(6692):439–447, Jul 1998. ISSN 1476-4687. doi: 10.1038/28792.

T. M. Lenton, M. Crouch, M. Johnson, N. Pires, and L. Dolan. First plants cooled the ordovician. *Nature Geoscience*, 5:86–89, 2 2012. ISSN 17520894. doi: 10.1038/ngeo1390.

J. E. Lovelock and L. Margulis. Atmospheric homeostasis by and for the biosphere: the gaia hypothesis. *Tellus*, 26:2–10, 1 1974. ISSN 0040-2826. doi: 10.3402/tellusa.v26i1-2.9731.

F. K. Lutgens and E. J. Tarbuck. *The Atmosphere: An introduction to meteorology.* Pearson, 8 edition, 2001. ISBN 9780130879578.

T. W. Lyons, C. T. Reinhard, and N. J. Planavsky. The rise of oxygen in earth's early ocean and atmosphere. *Nature*, 506:307–315, 2014. ISSN 00280836. doi: 10.1038/nature13068.

S. N. Mahapatro, N. C. Pant, S. K. Bhowmik, A. K. Tripathy, and J. K. Nanda. Archaean granulite facies metamorphism at the singhbhum craton-eastern ghats mobile belt interface: Implication for the ur supercontinent assembly. *Geological Journal*, 47:312–333, 2012. ISSN 10991034. doi: 10.1002/gj.1311.

A. C. Maloof, S. M. Porter, J. L. Moore, F. O. Dudas, S. A. Bowring, J. A. Higgins, D. A. Fike, and M. P. Eddy. The earliest cambrian record of animals and ocean geochemical change. *Geological Society of America Bulletin*, 122:1731–1774, 11 2010. ISSN 0016-7606. doi: 10.1130/B30346.1.

J. Manners, J. M. Edwards, P. Hill, and J.-C. Thelen. Socrates (suite of community radiative transfer codes based on edwards and slingo) technical guide., 2015. URL `https://code.metoffice.gov.uk/trac/socrates`.

N. J. Mayne, I. Baraffe, D. M. Acreman, C. Smith, N. Wood, D. S. Amundsen, J. Thuburn, and D. R. Jackson. Using the um dynamical cores to reproduce idealised 3-d flows. *Geoscientific Model Development*, 7:3059–3087, 12 2014. ISSN 19919603. doi: 10.5194/gmd-7-3059-2014.

N. J. Mayne, F. Debras, I. Baraffe, J. Thuburn, D. S. Amundsen, D. M. Acreman, C. Smith, M. K. Browning, J. Manners, and N. Wood. Results from a set of three-dimensional numerical experiments of a hot jupiter atmosphere. *Astronomy and Astrophysics*, 604, 8 2017. ISSN 14320746. doi: 10.1051/0004-6361/201730465.

N. J. Mayne, B. Drummond, F. Debras, E. Jaupart, J. Manners, I. A. Boutle, I. Baraffe, and K. Kohary. The Limits of the Primitive Equations of Dynamics for Warm, Slowly Rotating Small Neptunes and Super Earths. *Astrophys. J.*, 871(1):56, Jan 2019. ISSN 1538-4357. doi: 10.3847/1538-4357/aaf6e9.

D. McCulloch, N. Mayne, M. Bate, and D. Sergeev. Modelling an idealised martian climate with the unified model: The next "giant leap" for mars gcms., 2021. URL `https://meetingorganizer.copernicus.org/EPSC2021/EPSC2021-232.html`. 15th Europlanet Science Congress.

R. D. Nance, J. B. Murphy, and M. Santosh. The supercontinent cycle: A retrospective essay. *Gondwana Research*, 25:4–29, 2014. ISSN 1342937X. doi: 10.1016/j.gr.2012.12.026.

N. Nhleko. *The Pongola Supergroup in Swaziland*. PhD thesis, Rand Afrikaans University, 2003.

A. E. Nicholson, D. M. Wilkinson, H. T. P. Williams, and T. M. Lenton. Gaian bottlenecks and planetary habitability maintained by evolving model biospheres: The exogaia model. *Monthly Notices of the Royal Astronomical Society*, 477:727–740, 3 2018. doi: 10.1093/mnras/sty658. URL `http://arxiv.org/abs/1803.08063http://dx.doi.org/10.1093/mnras/sty658`.

R. Ojakangas and V. S. Hegde. The talya conglomerate: An archean ($\sim$ 2.7 ga) glaciomarine formation,western dharwar craton, southern india. *Current Science*, 106:387–396, 2014. URL `https://www.researchgate.net/publication/285982138`.

M. Oosterloo. The role of plate tectonics in the long-term evolution of atmospheric carbon dioxide content on earth-like exoplanets. Master's thesis, University of Groningen, 2020.

M. Oosterloo, D. Höning, I. E. Kamp, and F. F. V. D. Tak. The role of planetary interior in the long-term evolution of atmospheric co2on earth-like exoplanets. *Astronomy and Astrophysics*, 649, 5 2021. ISSN 14320746. doi: 10.1051/0004-6361/202039664.

J. Parnell and C. Brolly. Increased biomass and carbon burial 2 billion years ago triggered mountain building. *Communications Earth & Environment*, 2, 12 2021. doi: 10.1038/s43247-021-00313-5.

R. C. Payne, D. Brownlee, and J. F. Kasting. Oxidized micrometeorites suggest either high pco 2 or low pn 2 during the neoarchean. *Proceedings of the National Academy of Sciences*, 117: 1360–1366, 2020. doi: 10.1073/pnas.1910698117/-/DCSupplemental.

J. D. Piper. Protopangaea: Palaeomagnetic definition of earth's oldest (mid-archaean-palaeoproterozoic) supercontinent. *Journal of Geodynamics*, 50:154–165, 9 2010. ISSN 02643707. doi: 10.1016/j.jog.2010.01.002.

B. Sauterey, B. Charnay, A. Affholder, #. Stéphane Mazevet, and #. Régis Ferrière. Co-evolution of primitive methane-cycling ecosystems and early Earth's atmosphere and climate. *Nat. Commun.*, 11(1):2705., Jun 2020. ISSN 2041-1723. doi: 10.1038/s41467-020-16374-7.

G. Schubert, D. L. Turcotte, and P. Olson. *Mantle Convection in the Earth and Planets*. Cambridge University Press, 9 2001. ISBN 9780521353670. doi: 10.1017/CBO9780511612879.

N. Sleep. Plate tectonics through time. *Treatise on Geophysics - Volume 9: Evolution of the Earth*, pages 145–169, 2007. doi: 10.1016/B978-044452748-6/00143-7. URL `https://linkinghub.elsevier.com/retrieve/pii/B9780444527486001437`.

N. H. Sleep and K. Zahnle. Carbon dioxide cycling and implications for climate on ancient earth. *Journal of Geophysical Research E: Planets*, 106:1373–1399, 2001. ISSN 01480227. doi: 10.1029/2000JE001247.

A. Staniforth and N. Wood. The deep-atmosphere euler equations in a generalized vertical coordinate. *Monthly Weather Review*, 131:1931–1938, 2003.

A. Staniforth and N. Wood. Aspects of the dynamical core of a nonhydrostatic, deep-atmosphere, unified weather and climate-prediction model. *Journal of Computational Physics*, 227:3445–3464, 3 2008. ISSN 00219991. doi: 10.1016/j.jcp.2006.11.009.

D. J. Stevenson, T. Spohn, and G. Schubertt. Magnetism and thermal evolution of the terrestrial planets. *ICARUS*, 54:466–489, 1983.

E. Tajika and T. Matsui. Evolution of terrestrial proto-co 2 atmosphere coupled with thermal history of the earth. *Earth and Planetary Sctence Letters*, 113:251–266, 1992.

G. K. Vallis. *Atmospheric and Oceanic Fluid Dynamics*. Cambridge University Press, 2017. ISBN 9781107588417. doi: 10.1017/9781107588417.

J. C. Walker, P. B. Hays, and J. F. Kasting. A negative feedback mechanism for the long-term stabilization of earth's surface temperature. *Journal of Geophysical Research*, 86:9776–9782, 1981. ISSN 01480227. doi: 10.1029/JC086iC10p09776.

D. Walters, A. J. Baran, I. Boutle, M. Brooks, P. Earnshaw, J. Edwards, K. Furtado, P. Hill, A. Lock, J. Manners, C. Morcrette, J. Mulcahy, C. Sanchez, C. Smith, R. Stratton, W. Tennant, L. Tomassini, K. V. Weverberg, S. Vosper, M. Willett, J. Browse, A. Bushell, K. Carslaw, M. Dalvi, R. Essery, N. Gedney, S. Hardiman, B. Johnson, C. Johnson, A. Jones, C. Jones, G. Mann, S. Milton, H. Rumbold, A. Sellar, M. Ujiie, M. Whitall, K. Williams, and M. Zerroukat. The met office unified model global atmosphere 7.0/7.1 and jules global land 7.0 configurations. *Geoscientific Model Development*, 12:1909–1963, 5 2019. ISSN 19919603. doi: 10.5194/gmd-12-1909-2019.

G. E. Williams. Geological constraints on the precambrian history of earth's rotation and the moon's orbit. *Reviews of Geophysics*, 38:37–59, 2 2000. ISSN 87551209. doi: 10.1029/1999RG900016.

B. F. Windley, T. Kusky, and A. Polat. Onset of plate tectonics by the eoarchean. *Precambrian Research*, 352, 1 2021. ISSN 03019268. doi: 10.1016/j.precamres.2020.105980.

M. J. Wit and H. Furnes. Climatology: 3.5-ga hydrothermal fields and diamictites in the barberton greenstone belt-paleoarchean crust in cold environments. *Science Advances*, 2, 2 2016. ISSN 23752548. doi: 10.1126/sciadv.1500368.

N. Wood, A. Staniforth, A. White, T. Allen, M. Diamantakis, M. Gross, T. Melvin, C. Smith, S. Vosper, M. Zerroukat, and J. Thuburn. An inherently mass-conserving semi-implicit semi-lagrangian discretization of the deep-atmosphere global non-hydrostatic equations. *Quarterly Journal of the Royal Meteorological Society*, 140:1505–1520, 2014. ISSN 1477870X. doi: 10.1002/qj.2235.

A. Zhuravlev and R. Riding, editors. *The Ecology of the Cambrian Radiation*. Columbia University Press, 12 2000. ISBN 9780231106139. doi: 10.7312/zhur10612.

Appendix A

Temperature maps for the three scenarios

Figures A.1, A.2 and A.3 show the surface temperatures across the globe for the three scenarios shown in Table 2.3 and the three moments in the Archean.

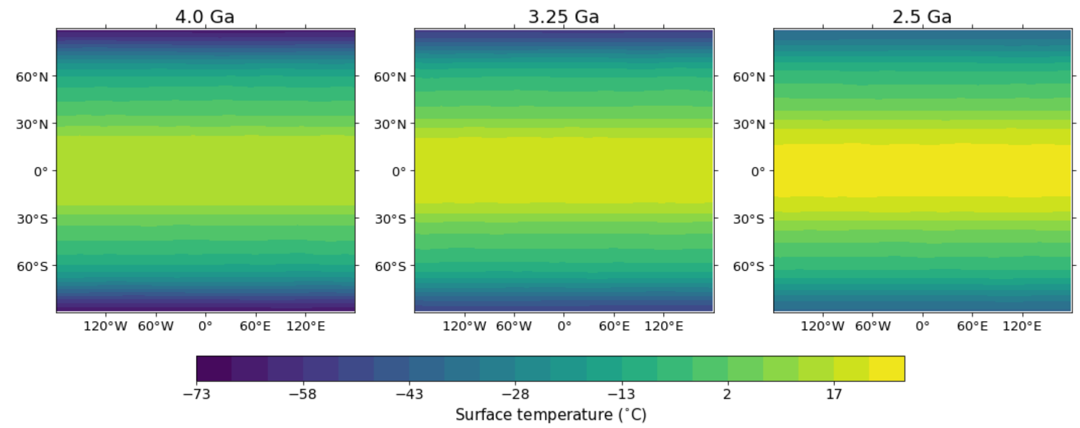

Figure A.1: Surface temperature for increasing solar luminosity, without thermal evolution and carbon cycle (LumChange)

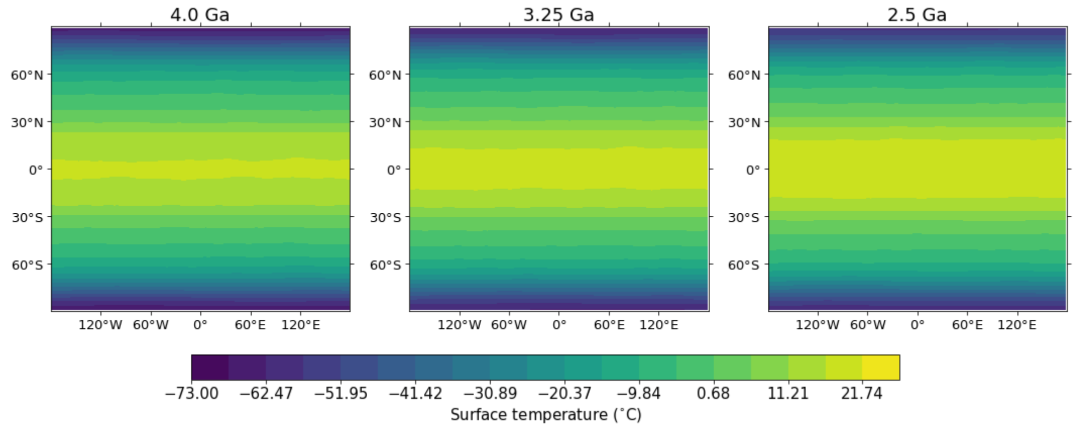

Figure A.2: Surface temperature for increasing solar luminosity, with thermal evolution and carbon cycle (BothChange)

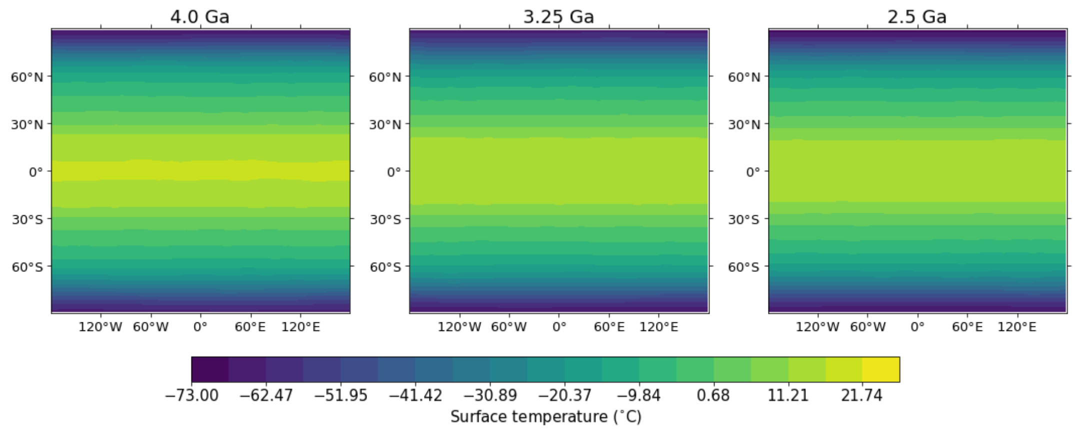

Figure A.3: Surface temperature for constant solar luminosity, with thermal evolution and carbon cycle (CO2Change)

Appendix B

Temperature change for all processes

Figures B.1, B.2, B.3 and B.4 show the change in temperature due to all heating and cooling processes as a function of altitude at the poles (B.1 and B.2) and at the equator (B.3 and B.4) for the LumChange and BothChange scenarios mentioned in Table 2.3 and for the three moments in the Archean.

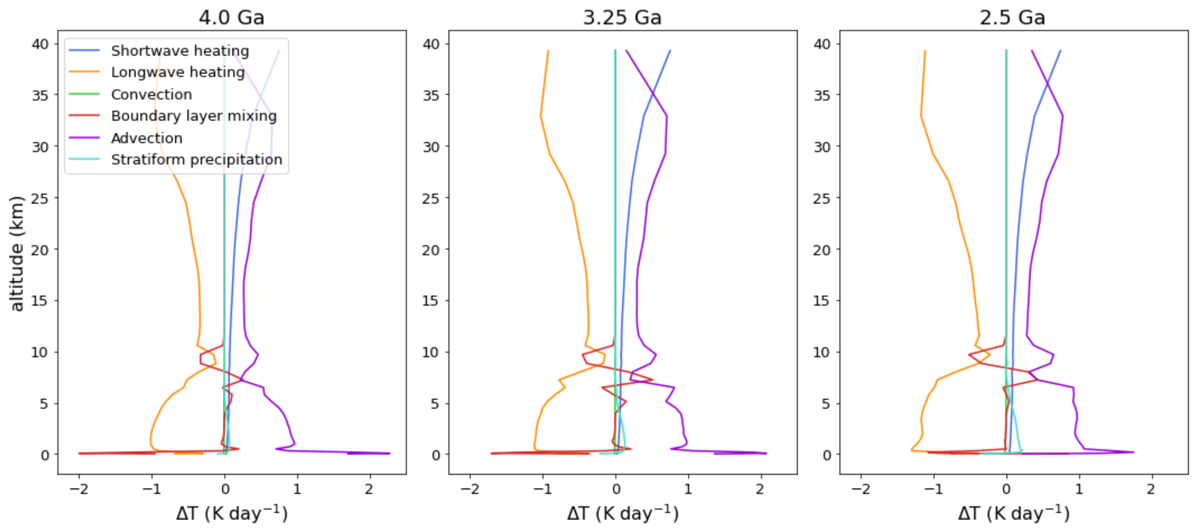

Figure B.1: Change in temperature due to various processes at the poles, for increasing solar luminosity and constant CO_2 levels (LumChange)

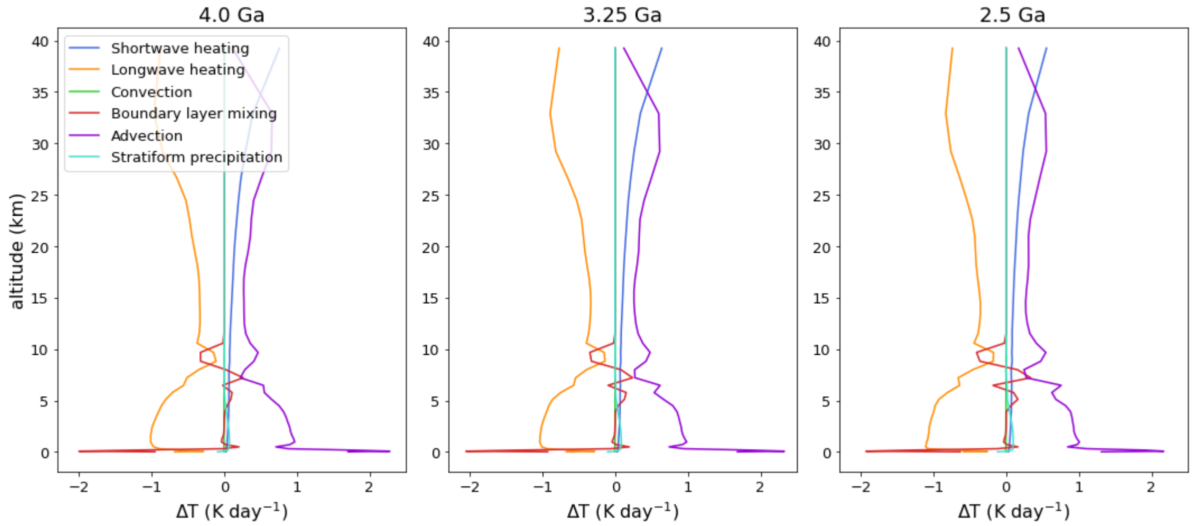

Figure B.2: Change in temperature due to various processes at the poles, for increasing solar luminosity and decreasing CO_2 levels (BothChange)

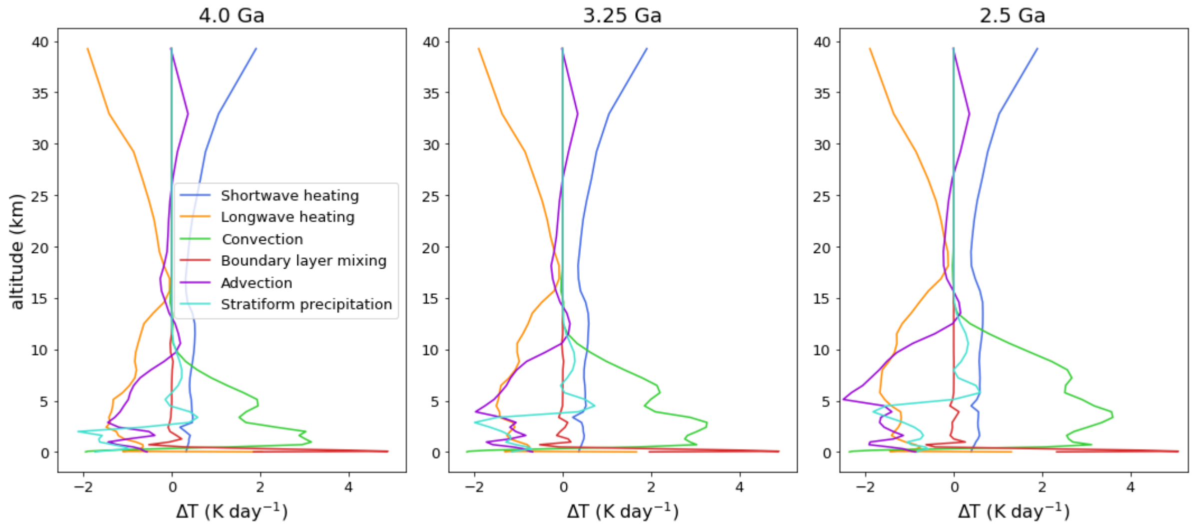

Figure B.3: Change in temperature due to various processes at the equator, for increasing solar luminosity and constant CO_2 levels (LumChange)

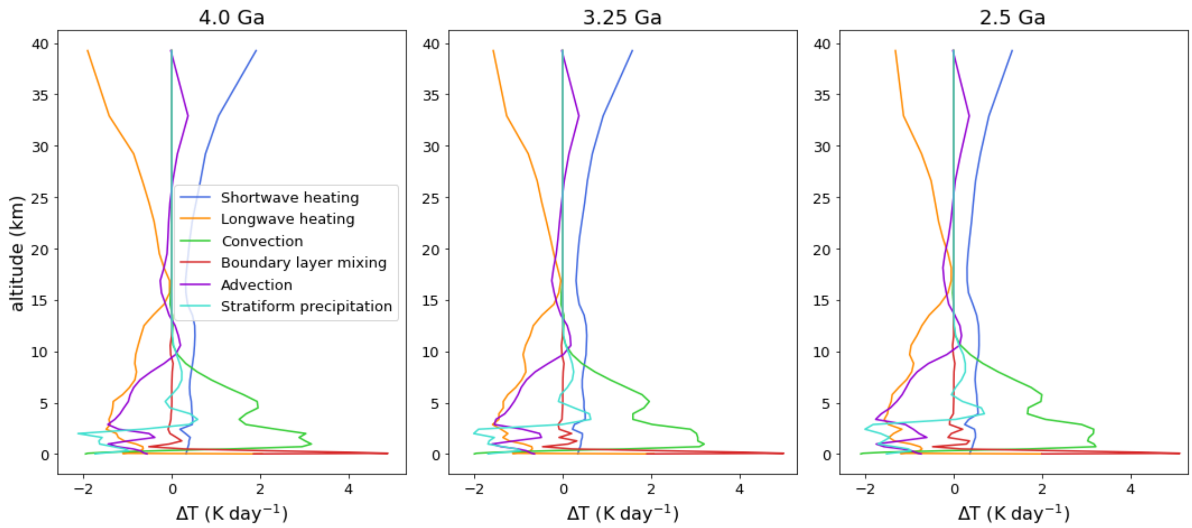

Figure B.4: Change in temperature due to various processes at the equator, for increasing solar luminosity and decreasing CO_2 levels (BothChange)